This is an accepted manuscript of an article published in Marine Geology.

The paper was first submitted on 29th May 2015.

The paper was accepted on 31st August 2015.

DOI: 10.1016/j.margeo.2015.08.021

Late Quaternary evolution and sea-level history of a glaciated marine embayment, Bantry Bay, SW Ireland

Ruth M.K. Plets[a,*], S. Louise Callard[b], J. Andrew G. Cooper[a], Antony J. Long[b], Rory J. Quinn[a], Daniel F. Belknap[c], Robin J. Edwards[d], Derek W.T. Jackson[a], Joseph T. Kelley[c], David Long[e], Glenn A. Milne[f], Xavier Monteys[g]

[a] School of Environmental Sciences, Ulster University, Coleraine BT52 1SA, UK

[b] Department of Geography, Durham University, Durham DH1 3LE, UK

[c] School of Earth and Climate Sciences, University of Maine, Orono ME 04469-5790, USA

[d] School of Natural Sciences, Trinity College Dublin, Dublin 2, Republic of Ireland

[e] British Geological Survey, West Mains Road, Edinburgh, EH9 3LA, UK

[f] Department of Earth Sciences, University of Ottawa, Ottawa ON, K1N 6N5, Canada

[g] Geological Survey of Ireland, Dublin 4, Ireland

[*] Corresponding author: r.plets@ulster.ac.uk

Abstract

Ireland experienced a spatially complex pattern of relative sea-level (RSL) changes and shoreline development caused by the interplay of isostatic and eustatic (ice equivalent sea level) processes since the Last Glacial Maximum (LGM). Using a combination of high-resolution marine geophysical data, vibrocores, foraminiferal analysis and 10 AMS radiocarbon dates, we reconstruct the Late Quaternary evolution and RSL history of Bantry Bay, a large (40 km long, 5-10 km wide) embayment in SW Ireland.

The data indicate two infill phases: one before and one after the LGM, separated by glacial and lowstand sediments. The pre-LGM history is not dated and the depositional history is inferred. A large sediment lobe formed at the outer edge of Bantry Bay as a lowstand ice-proximal glacimarine outwash system as the ice retreated after the LGM, at a sea level ca. 80 m lower than present. Iceberg scour immediately west of this location likely relate to the break-up of the local Kerry-Cork Ice Cap. Long curvilinear ridges, seen both offshore and on top of the sediment lobe, probably formed as shoreface ridges under stronger-than-present tidal currents during a period of RSL stability (pre– 14.6 ka cal BP). A subsequent infill phase is characterised by a basin-wide erosional (ravinement) surface and the deposition of inter- and sub-tidal estuarine sediments. Although our data support the general trends, our stratigraphic and radiocarbon data suggest a higher sea level between 11 and 13.5 ka cal BP than predicted by existing glacial isostatic adjustment models.

Keywords

Relative sea-level change; post-glacial transgression; multibeam echosounder; seismo-stratigraphy; litho-stratigraphy; Bantry Bay

Highlights

- We present multibeam, seismic profile and core data from a drowned marine inlet.

- Pre- and post-LGM sediments are preserved, separated by a glacial diamict.

- A tidal ravinement surface that post-dates a diamict deposit is widespread.

- Dating suggests the transgression reached the inner Bay before 13 ka cal BP.

- A mismatch exists between our radiocarbon dates and existing GIA models.

1. Introduction

Ireland was largely covered by ice at the Last Glacial Maximum (LGM; defined as 26.5 – 19 ka BP; Clark et al., 2009). The interplay between isostatic rebound and eustatic (ice equivalent) sea-level during and after ice retreat varied due to regional differences in ice load and the pattern of deglaciation and, as a result, relative sea-level (RSL) patterns are geographically highly varied. Recent glacio-isostatic adjustment (GIA) models predict such complexity in RSL around Ireland (Brooks et al., 2008; Bradley et al., 2011). According to these models, any location on the Irish coast would have experienced a lower than present RSL at some point after deglaciation, with the SW corner of Ireland predicted to have the lowest potential RSL (75 m below present sea level around 18 ka BP (Brooks et al., 2008). GIA models for SW Ireland (distant from the regional centre of the British and Irish Ice sheet (BIIS) loading over Scotland), for example, predict overall RSL rise from a LGM lowstand between ca. 20 – 14.6 ka cal BP (Figure 1). The start of this predicted RSL rise coincides with meltwater pulse 1A (MWP-1A: 14.65 to 14.31 ka cal BP (Deschamps et al., 2012)).

Such GIA models typically use an ice history model, a sea-level model and earth model, with each of these exhibiting a degree of uncertainty. Firstly, despite improved understanding of the dimensions of the western portion of the BIIS (e.g., Ó Cofaigh et al., 2012b; Dunlop et al., 2010; Clark et al., 2012), there is still uncertainty about the extent, thickness and history of the ice-sheet. Secondly, there are large gaps in the RSL data around Ireland. Brooks and Edwards (2006) tried to address this by compiling a database of sea-level information for Ireland (freely available from: http://www.naturalscience.tcd.ie/SL_Database.php). Such a database is crucial for comparing model output and field data, and thus constraining GIA models. A brief analysis of this dataset reveals that of the 45 primary index points, none are younger than 10 ka cal BP and most are from depths shallower than 5 m below water depth. From the 10 secondary index points, which are less precise indicators, only one is older than 10 ka BP and is the only one retrieved deeper than the intertidal zone; this sample was collected in Bantry Bay at a depth of -60 m (this data point will be discussed

later in this paper). Finally, from the 149 limiting dates, which only say whether RSL was above or below the dated level, 35 are older than 10 ka BP, but only 1 of these was recovered from a fully marine, offshore location. So, although there may be a reasonable fit between field data and modelled data for the Holocene, when RSL was only a few meters below or above the present sea-level, there are no real data for the Late-Pleistocene, when RSL was below present for many areas around Ireland. As a consequence, the GIA model predictions from this region are poorly constrained for periods when RSL was significantly lower than present because of a paucity of offshore data. This is the key time when uncertainties in the various ice, earth and eustatic models are at their greatest and, consequently, differences in GIA models are largest.

This study is the first in its kind in trying to address this gap in observational RSL data from offshore areas beyond the intertidal zone. Our approach concentrates on the integration of high-resolution marine geophysical data and core material to reconstruct the Late Quaternary evolution of Bantry Bay, an area where GIA models predict the lowest post-LGM lowstand in Ireland. We present new field data on the post-LGM RSL rise and compare these with GIA model predictions. Furthermore, this paper is the first step in the development of a seismo-stratigraphic model of the Late-Pleistocene to Early-Holocene along the Irish shelf.

2. Geological, oceanographic and Quaternary setting

Bantry Bay is an elongated marine inlet located in the Southwest of Ireland (Figure 2a). The Bay is 40 km long and narrows from 10 km between the Beara Peninsula and Sheep's Head to 5 km in the inner parts (Figure 2b). The bedrock geology of the area is dominated by Old Red Sandstone (Devonian), overlain by Uppermost Devonian and Carboniferous marine sandstones and mudstones (Pracht and Sleeman, 2002). The characteristic ENE-WSW aligned topography is caused by uplift and

folding during the Variscan Orogeny, with the synclines resulting in present-day valleys and the anticlines forming topographic highs.

The present seabed in Bantry Bay is relatively flat (slope < 1°) with water depths increasing gradually to 70 m, before dropping off more steeply (ca. 10°) at the mouth of the Bay into deeper water (ca. -100 m). Conditions are near fully marine (Edwards et al., 1996) with limited estuarine characteristics, even within the inner Bay (Roycroft et al., 2004). The tidal regime is semi-diurnal and is classified as meso-tidal (Edwards et al., 1996).

Recent studies demonstrate that during build-up to the LGM, ice reached the southern part of Ireland after 24 ka BP (the 'Irish Sea Till') (Ó Cofaigh et al., 2012a), with an ice stream that extended as far as the Scilly Isles (Hiemstra et al., 2006; Scourse et al., 2009a; McCarroll et al., 2010) (Figure 2a). Southwest Ireland remained under the influence of a local ice cap, the Kerry-Cork Ice Cap, centred on the Kenmare Valley, immediately north of Bantry Bay (Ballantyne et al., 2011) (Figure 2a). The presence of ice-moulded rock on the summit of Hungry Hill (685 m) implies ice thicknesses of >700 m flowing into Bantry Bay (Ballantyne et al., 2011). The lateral extent of the Kerry-Cork Ice Cap is marked by an outermost eastern moraine (Kilcummin and Killumney moraines) interpreted variously as the LGM limit, a post-LGM readvance (for discussion see Ballantyne et al. (2011)), or a recessional feature formed during the last deglaciation (Ó Cofaigh et al., 2012a). The offshore extent of the Kerry-Cork Ice Cap during the LGM is speculative. The maximum ice extent at the LGM appears short-lived. Two ^{36}Cl dates from low elevation sites near Kenmare and on the Sheep's Head Peninsula with reported ages of 22.0±3.4 and 21.3±1.3 ka BP, suggest early deglaciation of low ground in this area (Bowen et al., 2002). However, possible inheritance issues with cosmogenic dating means that this is a minimum age for deglaciation, whilst other reconstructions suggest that the local ice-cap was still present at 19 ka BP (Clark et al., 2012).

The RSL history of Bantry Bay reflects the combined influence of local and regional ice loading histories and the globally integrated ice volume signal expressed as variations in 'eustatic' sea level. Modelled RSL curves for west Cork (Figure 1) (Brooks et al., 2008; Bradley et al., 2011) use a common local ice sheet history for the BIIS, but differ slightly with regard to their Earth and non-local ice sheet models. The BIIS model (Brooks et al., 2008) is based on the reconstruction by Sejrup et al. (1994, 2005) and is additionally constrained by trim-line data (e.g. Ballantyne et al. 2006) which are interpreted as indicating maximum ice thickness. The model has an early phase of glaciation in which Ireland is largely covered by ice by 32 ka BP. Following a phase of retreat around 26 ka BP, the ice sheet expanded to its maximum lateral extent by 24 ka BP, extending onto the continental shelf and incorporating an ice stream from the Irish Sea as noted above. Rapid deglaciation after 21 ka BP left the study area ice-free by c. 18 ka BP. Whilst the timing and lateral extent of the modelled BIIS is broadly similar to more recent reconstructions (e.g. Clark et al., 2012), the reinterpretation of trimline data as englacial transitions between warm- and cold-based ice (i.e. minimum ice sheet thickness) opens up the possibility for increased loading terms in future modelling studies (e.g. Kuchar et al., 2012).

Modelled RSL curves for west Cork predict an initial lowstand, with stable RSL at depths between 72 and 78 m (below mean sea-level) for at least 5 ka, followed by a 20 m RSL rise between 14.6 and 13.5 ka cal BP (at a rate of c. 18 mm yr^{-1}) that reflects the impact of MWP-1A. This was followed by a slower rise of 8 m between 13.5 and 11 ka cal BP (3.2 mm yr^{-1}) after which there was a continued rise at reduced rates during the Holocene (Brooks et al., 2008; Bradley et al., 2011) (Figure 1). There are few dated sea-level index points in the area with which to test these models, and the majority of points are from water depths of -10 m or less. Indeed, the only offshore index point is described by Stillman (1968) as a black freshwater lake-floor deposit obtained from a borehole at ~ 57 m below Ordnance Datum. Relative dating of this deposit was based on pollen assemblages and was linked to pollen Zone II / Allerød (13 – 14 ka cal BP) (Stillman, 1968).

3. Methods

3.1. Geophysical data

Multibeam echosounder data (bathymetry and backscatter) were acquired as part of the INFOMAR Programme from the *RV Celtic Voyager, RV Celtic Explorer* and *SV Rocinante* between 2004 and 2007 using Kongsberg Simrad EM1002 and EM3002 systems. Bathymetric data were processed and cleaned by the Marine Institute of Ireland and subsequently gridded using QPS Fledermaus v.7 to 2 x 2 m resolution (Figure 2b). The backscatter data used in this study were processed in QPS FMGeocoder and also gridded to 2 x 2 m resolution (Figure 2c). Analysis of the resulting multibeam grids was performed in ESRI ArcGIS 9.2.

High-resolution pinger sub-bottom data (SES 5000 3.5 kHz hull-mounted) were acquired simultaneously alongside the multibeam data and recorded on a CODA system. Post-processing was performed in IHS Kingdom 8.8, which involved tidal correction to lowest astronomical tide (LAT), trapezoid band-pass filtering (1.8 – 2.0 – 6.0 – 6.2 kHz), automatic gain control (10, 20 and 50 ms) and wavelet envelope calculation. In total, 269 seismic lines were considered to be of sufficient quality to be included in the analysis, with line spacing varying from 75 m in the inner parts of the Bay, to over 750 m for the most seaward lines. In addition, a sparker line (towed Geo-Spark 200 system, dominant frequency between 0.5 – 2 kHz) acquired by the Geological Survey of Ireland in the inner part of Bantry Bay in 2007 was incorporated and processed using IHS Kingdom software (trapezoid band-pass of 0.4 – 0.5 – 2.0 – 2.5 kHz and automatic gain control of 50 and 100 ms). Seismic interpretation was performed in IHS Kingdom and all seismic-derived surfaces/grids were created using the Flex Gridding algorithm with a 20 x 20 m cell size. These grids were subsequently imported and analysed in ESRI ArcGIS 9.2. Where seismic depths or acoustic unit thicknesses have been converted from two-way travel time to metres, an acoustic interval velocity of 1550 m/s was

chosen. Core logs were imported and superimposed onto the seismic data using a linear velocity model of 1550 – 1700 m/s over a core length of 6 m in IHS Kingdom Software.

3.2. Core material

On June 10th and 11th 2012, 25 stations were cored using a GeoResources (6 m barrel, 11 cm diameter PVC liner) vibrocorer deployed from *RV Celtic Explorer* (Figure 3). DGPS positioning and water depth were recorded manually; water depths were later adjusted to multibeam water depths (LAT), approximately 1.6 m below mean sea-level (POLPRED UKCS model). Core-length recovery varied from just a few centimetres in the outer Bay to 5.45 m in the inner Bay (Figure 3, Appendix 1). Cores were stored horizontally during transit and placed in refrigerated facilities (4°C) after disembarkation. All cores were split, photographed and described (lithology, texture, contacts, sedimentary structures and Munsell colour).

Samples for radiocarbon dating were collected at stratigraphically significant horizons. Each sample was wet sieved on 500 and 63 µm sieves, with the coarse and fine fraction retained. Using a light-reflecting microscope, foraminifera in the fine fraction were wet picked, identified, and dried in an oven at 40°C. Monospecific foraminifera samples were used for dating only as no shells were present. In some instances larger foraminifera species were picked over the most abundant species due to their size and thus providing enough material for dating (e.g. *Planorbulina mediterraneansis*), which the abundant smaller species would not be able to. Monospecific benthic foraminifera samples of *Quinqueloculina seminulum*, *Elphidium excavatum* and *Planorbulina mediterranensis*, were selected for Accelerator Mass Spectrometry (AMS) ^{14}C dating (Table 1) at the SUERC Radiocarbon Dating Laboratory. Two samples, ranging from 200µm to 350µm carbon, were analysed by AMS at low current at the Keck C cycle AMS Lab, University of California. Samples were hydrolysed with 100% orthophosphoric acid at 25°C, and the generated CO_2 converted to graphite by Fe/Zn reduction. The graphite stubs were then analysed by ^{14}C AMS. The conventional ages were

calibrated using the Marine13 curve (Calib v.7.0.2, Reimer et al., 2013), and corrected for the local reservoir effect of δR of -55 ± 42 according to the values obtained from the marine reservoir correction database (QUB ^{14}Chrono Centre, 2013; Harkness, 1983; Blake, 2005; Butler et al., 2009). Dates are reported as mean (2 sigma range) calibrated calendar years before present (ka cal BP) unless otherwise stated.

Foraminifera were extracted from five cores to produce a comparative biostratigraphy for the inner and outer Bay cores. A 3 cc volume of sample was wet sieved over 63 µm, 125 µm and 500 µm sieves. A minimum of 300 foraminifera were handpicked from the 500-125 µm fraction. The foraminifera preservation, including whether the test was broken, abraded or pyritized was noted. Identifications were based on various taxonomic references (Appendix 2) (e.g. Haynes, 1973; Murray, 1971; 1979; 1991; 2003; Nooijer et al., 2008).

4. Results

4.1. Multibeam data

The study area can be sub-divided into three zones: (1) the inner Bay, running from the upper reaches of the Bay to Sheep's Head, (2) the outer Bay, where the Bay widens and is joined by the outlet of Dunmanus Bay and (3) the offshore region (Figure 2c).

The seabed in the inner Bay slopes gently (< 1°) seaward and is bounded by steep sides. Backscatter data indicate the perimeter of the Bay is bedrock (high backscatter), and the interior is filled with sediment (lower backscatter) (Figure 2c).

At the mouth of the Bay, the seabed flattens at depths around 70 m, before dropping off more steeply to water depths of 120 m. Seaward of this break in slope, the seafloor gradually descends to 200 m. The backscatter signature in the outer Bay is higher than the inner Bay and offshore region, suggesting the presence of coarser material.

A series of long (up to 22 km), parallel and symmetrical ridges are present at the mouth of the Bay (full arrows Figure 2 b and c; see Figure 4 A for detail and profile). The deepest (129 to 131 m) ridge extends for 22 km, is less than 2 m high and curves around the exposed bedrock off the tip of the Beara Peninsula (Figure 4 A3-4). Closer inshore, between 96 and 108 m water depth, similar parallel ridges up to 9 km long, with a maximum height and width of 2 m and 1 km, respectively, are imaged. Shorter, more localised ridges are present in water depths between 80 and 88 m. These ridge features are imaged as a series of contrasting high-and low-backscatter lineations. Just to the south-west of the deepest, longest ridges, criss-crossing km-long furrow-like scour marks are present in water depths around 140 to 150 m, but can only be detected on the backscatter data (Figure 4 A2). Further east, to the south of Dunmanus Bay, the highest ridge has a positive relief of up to 20 m in water depths between 70 and 90 m (broken arrow Figure 2 b and c). This feature extends for 9 km and is 1 km wide and, in contrast to the other ridges, this feature is isolated and characterised by very low backscatter values (Figure 2 c).

Inshore from the ridges, and to the south of the most westerly tip of the Beara Peninsula, a scarp with a maximum height of 10 m is present between 76 m and 93 m water depth (dotted-broken arrow Figure 2 b–c; see Figure 4 B for detail and profile). The gradient of this scarp varies from c. 0.5° along its northern section, to c. 4° in the middle section and c. 2° along the southern section. There is a strong contrast in the backscatter intensity between the bottom of the scarp (high backscatter, suggesting coarse material), the slope area (low backscatter) and the top of the plateau (low to medium backscatter) (Figure 4 B2). The scarp and the deepest long ridges form the edge of a large sediment lobe (blue area in Figure 4 B3) located at the outer part of the Bay mouth.

Whilst the offshore region is a largely featureless slope characterised by low backscatter, in the deepest parts, close to the eastern edge of the Porcupine Seabight (below water depths of 175 m),

linear intersecting km-long features are imaged (Figure 4 C) with an average scour depth of 1 m (Figure 4 C4) . The backscatter data show pockets of high intensity associated with these (Figure 4 C2). These are similar to the lineations found to the southwest of the longest curvilinear ridges.

4.2. Seismo-stratigraphy

Six units are interpreted from the pinger and sparker seismic data, separated by five bounding surfaces (Figures 5 and 6).

Unit 1 (U1): This is the deepest unit visible on the seismic data and, as such, is considered to be the acoustic basement. Surface S1, which overlies U1, is characterized by a high-amplitude continuous reflector. This surface is topographically variable, and divides the Bay into a series of large basins and ridges. The Unit itself consists of discontinuous, low amplitude chaotic reflectors. It is easier to detect on the lower frequency sparker dataset than on the higher frequency pinger data.

Unit 2 (U2): This unit is bound by the high-amplitude reflector S1 at the base, and a mostly continuous, medium amplitude reflector S2 at the top. This unit comprises (sub)parallel reflectors, onlapping onto the underlying S1. The top of the unit is truncated by S2 in the Inner Bay, whilst towards the Outer Bay, S2 appears more conformable. The unit fills the deepest basement troughs and is confined to these deeper areas.

Unit 3 (U3): The medium amplitude reflector S2 forms the base of this unit. The top bounding surface, S3, is characterized by a mostly continuous relatively high amplitude reflector. The unit is divided into three sub-units based on the sparker data (U3a, U3b and U3c). The bottom sub-unit, U3a, is predominantly transparent. A more contorted and chaotic unit (U3b) overlies this. It contains some clear diffraction hyperbolae, and forms highs. These highs usually occur in several parallel seismic lines, and as such, can be defined as ridges. These ridges usually have a flat-topped

appearance (Figure 6) and are orientated NW-SE, perpendicular to the main axis of the bay. Except for the areas with the ridges, this unit is in turn covered by a transparent unit, U3c, which is acoustically similar to U3a. On many of the pinger profiles this unit forms the acoustic basement, indicating that the top of the unit is almost impenetrable for the high frequency source. The chaotic nature of the underlying unit makes it difficult to see whether Surface S3 truncates U3.

Unit 4 (U4): The medium-high, mostly continuous S3 surface is found at the base of this unit. In contrast, the top bounding reflector S4 appears disrupted and discontinuous, and clearly truncates the underlying unit. Whilst the surface is easily traceable on the sparker data, on the pinger profiles it is often very disrupted and hummocky, and more difficult to trace laterally. The unit itself is characterised by a series of low amplitude reflectors, giving it an almost transparent appearance. These reflectors do, however, often show a wavy or lenticular configuration. This unit is usually absent from the top of the U3b ridges, but occurs as a prograding facies, infilling troughs in the underlying unit. Some channels occur within this unit (up to 250 m wide in the shallower parts of the Bay, but up to 500 m wide in deeper areas). These channels are vertically stacked (predominantly laterally offset) (Figure 6), are mainly concentrated towards the top of the unit and have not been observed on seismic data outside the inner Bay area.

Unit 5 (U5): Above the discontinuous surface S4, Unit 5 is found. An equally discontinuous and disrupted, but higher amplitude, surface S5 forms the top of the unit. Towards the sides of the basin, S5 merges with S4 into a single surface, suggesting that U5 becomes very thin at the edges or disappears. U5 exists in the enveloped pinger data as a dark turbid unit. When the envelope is removed from the pinger data, discontinuous reflectors and some diffraction hyperbolae are imaged. On the sparker data, the unit consists of parallel but discontinuous reflectors. Some of the channels imaged in the upper part of U4 appear to migrate up into the lower section of U5 (Figure

6). The disrupted nature of Surface S5, paired with the chaotic reflectors of U5 make it difficult to determine whether this surface is erosional or conformable.

Unit 6 (U6) is imaged below the seabed surface and above S5. The Unit is divided into two sub-units (U6a and U6b), that can only be differentiated on the pinger data. The lower sub-unit, U6a, is characterized by parallel continuous reflectors which appear to be infilling (basin-scale) depressions on top of Unit 5. This is overlain by a very low amplitude sub-unit (U6b) with only occasional stronger amplitude reflectors, and forms the current seabed. In addition to the horizontal units, vertical 'pillar'-like turbid zones are imaged in Unit 6 (so-called Acoustic Turbidity Zones), with acoustically transparent zones directly beneath.

4.3. Litho- and biostratigraphy (see reviewer 2 comment)

Based on sedimentology and analysis of the foraminifera (Appendix 2), six bio-lithofacies (A-F) were identified (Table 2; Figure 3, 7 and 8; Appendix 2 and 3):

Bio-lithofacies F is made up of dark grey fine-to-medium sand with no or few shell fragments. It was not cored in the outer parts of the Bay. In some of the cores, a fining (F1) or coarsening (F2) upwards trend is noted. This facies often contains abundant organic material including *Chenopodium* and *Menyanthes* species. Three foraminifera samples from two cores (BB2 and BB6) were taken from bio-lithofacies F. In BB2, Cas*sidulina obtusa* (34-42%) dominates the foraminifera assemblage together with a significant abundance of *Haynesina germanica* (14-20%)*, Cibicides lobatulus* (15%) and *Elphidium excavatum* (11%). In BB6 *Milliolinella subrotundra* (14%) co-dominates with *C. obtusa* (10%) and *C. lobatulus* (9%)*;* this composition is largely the same for facies D. The proportion of broken test is between 21-29% with *C. obtusa* and *E. excavatum* having 8-10% and 6% broken test, respectively; *H. germanica* has very low proportion of broken tests.

Bio-lithofacies E was recovered in three cores and is a coarse grained unit consisting of well-rounded (predominantly slate, bladed) pebbles. The contact with the overlying unit is sharp. This facies was analysed for foraminifera in one core (BB23) where it was dominated by *Bulimina* types (22-33%; infaunal)*, C. lobatulus* (12-20%; epifaunal), *Quinqueloculina* sp. (13-17%; epifaunal) and *C. laevigata* (14-15%; infaunal). The concentration of foraminifera tests for these samples is high with 33-46% of the test broken.

Bio-lithofacies D is composed of a series of finely-laminated grey to dark grey clay and sand layers. Fine organic material including seeds of *Chenopodium* and *Menyanthes*, bioturbation and flaser bedding occur within this unit, which was only encountered in the inner part of the Bay. Shell fragments and larger shells occur in relatively low abundance. Four foraminifera samples, one from the outer bay (BB24) and three from the inner bay (BB1, BB2 and BB6) were analysed. For all four samples, foraminifera concentrations were generally lower compared to the other facies. The three inner bay samples are dominated by either *C. obtusa* (35% and 20% for BB2 and BB6 respectively) or *M. subrotundra* (22% in BB1). Other abundant species include *C. lobatulus* (8-16%), *Asterigerinata mamilla* (8-12%), *E. excavatum* (5-15%) and *H. germanica* (4-9%). This assemblage is similar to that described in bio-lithofacies F and combined with the abundance of organic material in bio-lithofacies D is likely to represent the same depositional environment as that proposed for bio-lithofacies F. The foraminiferal assemblage for the outer bay core, BB24, is very different: *Quinqueloculina* types dominate (18%) with *C. lobatulus* and *Bulimina* types secondary (11% and 10% respectively). *C. obtusa* (8%) and *A. mamilla* (7%) are also prominent. The proportion of broken foraminifera test range between 28-30%. The most common species with broken test for this lithofacies are *Asterigerinata mamilla* (2-5%), *Cassidulina obtusa* (2-10%), *Cibicides lobatulus* (3-4%) and *Elphidium excavatum* (2-8%). In both the inner and outer bay cores, the boundary between facies D and the overlying unit is usually sharp.

Bio-lithofacies C comprises medium-to-coarse dark grey sand with shell fragments and large broken shells and forms the seabed in some of the outer Bay areas. Where it underlies another facies, the boundary is usually gradual. It is found in only two cores (BB1 and BB6) in the inner Bay, where it contains some fine organic matter. Based on the lithology, this unit is composed of reworked material and, as such no micropalaeontological analysis was performed.

Bio-lithofacies B occurs in all parts of the Bay and is characterised by crudely-laminated, dark grey, fine-to-medium sand with clear shell hash layers (Bs). In some outer Bay cores this facies crops out on the seabed in the area near the interpreted scarp. Bio-lithofacies B was only sampled from one outer bay core (BB18). Foraminiferal concentrations reduce up-core, being very high at the base (920-614 test/1cc) and dropping to only 73 tests/1cc material at the top. The samples at the top also showed a large proportion (41%) of broken tests. The base of the core is dominated by *A. mamilla* (15-22%) and *M. subrotundra (16-19%),* with *C. lobatulus* (11-14%), *Quinqueloculina sp.* (9-10%) and *Planorbulina mediterranensis* (8%) secondary. The top of the core is dominated by *Quinqueloculina sp.* (31%) and the agglutinated species *T. sagittula* (22%) is secondary. Also present in high abundances is *C. lobatulus* (18%) and *C. laevigata* (11%).

Bio-lithofacies A represents the seabed in all cores located in the inner Bay, but is absent in the deepest cores. It is a dark grey fine sand, silty sand or silt with a relatively high abundance of shell fragments and shows no sedimentary structures, except for an occasional shell hash layer. Six samples from three cores provide foraminiferal assemblage data; two from the inner bay (BB2 and BB6) and one from the outer bay (BB24).The overall foraminifera count is high with a maximum concentration reaching 1710 tests per 1cc of material (from the top of BB6). Large assemblage changes between the two inner cores were observed. At the base, BB2 is dominated by *H. germanica* (26%), with *E. excavatum* (17%) and *M. subrotundra* (14%) secondary species. *E. excavatum* continues to be present in similar abundances as in the facies below, however, there is a

large reduction in the proportion of *C. obtusa* (4%). In BB6, the lower sample (190-191 cm) is dominated by *E. excavatum* (45%) with *Quinqueloculina sp* (10%) as secondary. The uppermost samples of both BB2 and BB6 are dominated by *Bulimina* types (43% and 38% respectively) with *C. lobatulus* (9%), *N. turgida* (8%) and *T. sagittula (8%)* being secondary in BB2 and *E. excavatum (13%)* and *Ammonia beccarii (13%)* secondary in BB6. The only core sampled in the outer bay (BB24), is also dominated by *Bulimina* types (56%) and has a similar foraminifera assemblage as BB6. The basal contact with underlying facies is usually sharp. The proportion of broken test range between 29-33% with the exception of a single sample from BB2 (55-56 cm) with only 12% broken test. This is the lowest proportion of broken test for all samples. The common species with broken test include *Ammonia becarrii* (6-8%), *Bullimina* species (9-11%) and, in BB6, *Elphidium excavatum* (17%).

4.4. Radiocarbon dates

The calibrated radiocarbon dates for ten samples, from three cores, are presented in Table 1. The oldest ages are from BB2 located in the inner Bay and are 11931 ± 47 ^{14}C a BP (13438 ± 151 cal a BP) and 11845 ± 46 ^{14}C a BP (13360 ± 131 cal a BP) for bio-lithofacies F and D respectively. These ages date seismic unit U4 (Figure 8). Three ages were collected from two cores (BB18 and BB24) in the outer Bay area. Two samples from BB18, the deepest core collected, date seismic units U5 and the base of U6 (10008 ± 45 ^{14}C a BP (11031 ± 175 cal a BP) and 10135 ± 30 ^{14}C a BP (11184 ± 115 cal a BP)) respectively. There is a small age reversal, although this is within the age errors of the two ages. The youngest age of 9331 ± 45 ^{14}C a BP (10258 ± 152 cal a BP) dates the base of BB24 and seismic unit U6. Although the samples are from different cores, they are in seismo-stratigraphic order, with the oldest ages from U4 and the youngest age from U6.

5. Data integration and interpretation

5.1. Multibeam data

The km-long crossing lineations resemble iceberg ploughmarks with associated pockets of ice-rafted debris (high backscatter) (e.g. Bellec et al., 2008; Hill et al., 2008). These are found in two separate areas (Figure 4 A and C), possibly indicating two distinct calving margins or different episodes of calving. North of the study area, iceberg scours are commonly found on the Western Irish shelf break in water depths between 230 and 590 m (Belderson et al., 1973; Sacchetti et al., 2012). Whilst the most westerly scour signature off Bantry Bay does occur fairly close to the shelf break adjacent to the Porcupine Seabight, the most easterly ploughmarks are found in shallower water (140 to 150 m water depth), positioned on the flat continental shelf and closer to the current coastline than any examples previously reported for this section of the shelf. Because of their location in shallower water and closer to the current coastline, we tentatively propose that these marks are linked to the retreat and calving of the local Kerry-Cork Ice Cap. Towards the east of these latter iceberg ploughmarks, the backscatter data show a mobile sand sheet partially draping these scour features (Figure 4 A1&A3), suggesting their original extent would have been further eastwards.

We consider three possible interpretations for the large linear ridges to the east of the iceberg ploughmarks, which in turn leads to different interpretations for the scarp off the Beara Peninsula headland. The first interpretation is that these are glacial features, possibly retreat moraines. While the size, depth and proximity of the iceberg scour signatures are consistent with such an interpretation, it would imply an ice lobe anchored on the headland, as opposed to flowing out of Bantry Bay, with the scarp potentially being a glacial feature. The fact that some of the ridges are very low (a few 10s of centimetres) and consistently linear, combined with the backscatter signature indicating that these are comprised of fine sediment with coarser material in the troughs is, however, inconsistent with a glacial origin (Figure 2c and 8 a&b). Morainal features preserved on the seabed would most likely have a higher relief and be composed of coarser material than the surrounding seabed (e.g. Stewart and Bradwell, 2014), with the troughs accumulating the finer material.

An alternative interpretation is that these straight and low-amplitude streamlined ridges are mega-scale glacial lineations, like those associated with ice streams draining large ice-sheet basins (Dowdeswell et al., 2008). Such lineations are typically formed parallel to the direction of the ice stream and this would imply an ice stream flowing parallel to the modern coastline, for which there is no other evidence along the Western Irish shelf. Furthermore, since iceberg scouring is seen to the west of these ridges, iceberg keel ploughing would also have left marks across the streamlined ridges during ice retreat if these were created by an ice stream. The unlikely ice-flow direction and the absence of iceberg scouring across the ridges, suggests that this interpretation is improbable.

The third possibility is that these features are bedforms created by tidal currents. Model predictions (Regional Ocean Modeling System, ROMS) of the present bottom current speed show locally increased velocity and reversing currents around the Beara Peninsula headland (ROMS data for Ireland is available from: http://www.marine.ie/Home/site-area/data-services/marine-forecasts/ocean-forecasts). However, modelling of palaeo-tidal currents (see Figure 3 in Scourse et al. (2009a)) suggests significantly larger (> 10 N/m^2) than present peak bed stresses (< 5 - 10 N/m^2) running around the southwest corner of Ireland in a northwest direction. These were active between 17 and 14 ka BP, just after the ice retreated, when sea level was lower and the coastline was located further seaward. Larger (5 - 10 N/m^2) than present peak bed stress was maintained until 8 or possibly 6 ka BP. Similar, but much larger linear sand ridges on the Celtic Sea shelf in water depths of 135 to 200 m have been interpreted as forming under larger than present tidal currents during the early stages of transgression between 20 and 12 ka BP (Scourse et al., 2009a). If the Bantry ridges are relict tidal bedforms, they effectively represent lowstand shoreface deposits. As tidal ridges typically form in water depths shallower than 50 m (Liu et al., 2007), then the deepest ridges (now at 130 m) formed at a time when RSL was at a depth of 80 - 130 m below present and the shallowest ridges (now at 80 m) when RSL was at a depth of 30 to 80 m. Such water depths would suggest that

the scarp, with its base between 76 m and 93 m water depth, could represent an erosional feature formed during this lowstand. The iceberg scour at depths below 140 m has remained unaffected, with just a thin rippled sand sheet moving over these, suggesting RSL did not drop below this depth. The rippled sand sheet, which can only be detected on the backscatter data, is interpreted to represent contemporary sediment movement, suggesting the larger ridges were indeed formed by stronger than present currents at a time of lower sea-level.

This interpretation poses the question of what the sediment source was for these proposed tidal ridges. In the case of the Celtic Sea ridges, reworked estuarine and deltaic lowstand facies have been suggested and accepted by most researchers to be the main sediment source, although a glacigenic origin has not been dismissed (see Scourse et al. (2009b) for a review and discussion). Accordingly, the core of the ridges off Bantry Bay could be of a glacial or post-glacial origin. Conversely, very strong tidal currents between 17 and 14 ka BP could also have reworked coast-parallel glacial features. Seismic lines through the larger ridge show an underlying high feature sitting on a flattened surface, with buried smaller ridges landward; these buried features are clearly distinct from the ridges exposed on the seabed (Figure 10 a-b-c). Where these underlying ridges are exposed on the contemporary seabed (i.e. in the troughs between the larger ridges) the backscatter indicates coarser material, with finer material making up the elevated ridges. The buried features, composed of coarser substrate, might therefore represent moraines. After the ice had retreated, these may have been reworked by strong tidal currents, winnowing the softer material from the tops of the former moraines and depositing this material as a series of curvilinear ridges aligned parallel to the former coastline. Conversely, during the early stages of deglaciation, large amounts of sediment would have accumulated at the Bay mouth as outwash, possibly deposited as an ice-proximal glacimarine outwash system (grounding line outwash fan or delta) (Lønne, 1995). The sediment lobe forming the flat plateau at the bay mouth could therefore be the expression of such a glacimarine outwash feature. As the tidal currents increased in strength after ice retreat, some of the outwash

material may have been reworked into tidal ridges, initially at the offshore end of the glacimarine system, and as sea level started to rise, on top of it.

Unfortunately none of the ridges have been cored and, as such, these interpretations can only be regarded as hypotheses. Although attempts were made to sample the scarp, all cores resulted in no recovery, which is suggestive of a coarse or compact substrate. This would support the interpretation that the glacimarine outwash system underwent erosion and reworking in a coastal setting, resulting in the development of a thin lag deposit.

Thus, the interpretation most supported by the evidence is of pre-existing depositional features (moraines and glacimarine fan/delta) being reworked by shoreface currents (to produce the ridges) and wave processes (to form the scarp and lag deposit) at a former sea level between 90 to 80 m below present sea level.

Finally, the isolated 20 m tall ridge to the south of Dunmanus Bay in water depths of 70 and 90 m (Figure 2 c; Figure 9 c), has an acoustic character very different from the long ridges discussed above. The backscatter is very low, indicating very soft sediment, and the seismic data show no internal or underlying structure. Possible explanations for this feature are a glacimarine outwash fan, or submerged shoreline feature (e.g. overstepped barrier). Again, ground-truthing is needed to test this interpretation.

5.2. Overall stratigraphy

The seismo-stratigraphic (Figure 5) and sedimentary facies analysis (Table 2) allows interpretation of several surfaces or units with respect to potential former shorelines and RSL. By superimposing the cores on the seismic sections (Figure 10), we see that U4 is the deepest unit cored. However, the majority of the inner Bay cores did not penetrate deeper than U5, and the cores rarely reach below

U6 in the outer part of the Bay. Based on the combination of the seismic and core datasets, seven stratigraphic units are identified (Table 3, Figure 8):

Unit VII: This unit is identified only from the seismic data (acoustic unit U1) and forms the acoustic basement. Where it crops out at the surface, multibeam bathymetric data reveal the cleaved and folded nature of the Old Red Sandstone (Pracht and Sleeman, 2002).

Unit VI: The deepest sedimentary unit (acoustic unit U2) is imaged only on the sparker data, where the parallel and onlapping nature of the reflectors of U2 indicate low energy sediment deposition in an estuarine or lacustrine environment. These sediments infilled bedrock depressions in the inner Bay. As the overlying Unit IV has been interpreted as a possible till (see below), Unit VI pre-dates a glacial phase. Pre-LGM deposits have occasionally survived glaciation in Ireland; for example, in West Cork, and along large stretches of the south coast of Ireland, a raised beach dated to MIS 4-3 (76 – 24 ka BP) is thought to have been deposited during a period of glacio-isostatic depression, combined with a high eustatic sea-level (Ó Cofaigh et al., 2012a). Alternatively, sediments assigned to the Gortian interglacial stage have been cored from Cork Harbour; the exact age of this stage is, however, still unresolved and could relate to either MIS 7, 9 or 11 (Dowling and Coxon, 2001). The age of U2 cannot be determined from seismic data alone, but the organic-rich silt deposit described by Stillman (1968) at a water depth of 57 m could correspond to the acoustic unit U2, and would thus be older than his suggested pollen Zone II / Allerød (13 – 14 ka cal BP) interpretation. Unfortunately, Stillman (1968) does not detail the specific pollen so it is not possible to examine the possibility that these could be of an earlier interglacial period.

Unit V: The sediments overlying Unit VI are identified from the seismic data as acoustic unitU3. They are either transparent or very contorted, suggesting rapid deposition of large amounts of sediments. Diffraction hyperbolae indicate the presence of boulders or blocks. The ridges formed by sub-unit

U3b display fault-like shear planes (Figure 6), implying the sediment has been deformed into ridges. All these features are consistent with interpretation of Unit IV as a glacial diamict, with the ridges representing possible push-moraines, deposited during the LGM. These push moraines were subsequently eroded to form a flat surface (S3), with the eroded sediments deposited in topographically low areas as Unit IV.

Unit IV: This unit correlates with acoustic unitU4. The lenticular configuration of the reflectors suggests deposition in shallow water. This unit is absent from the tops of the push-moraines but forms a prograding facies with oblique parallel clinoforms that infills the intervening topographic lows (Figure 6). The sediments comprising this unit are most likely glacial outwash sediments as well as paraglacial sediments formed through the reworking of glacial material.

Offshore, acoustic unitU4 comprises a large sediment lobe on a flat but irregular surface (S2) at the mouth of the Bay. The weak dipping reflectors in an offshore direction in some seismic sections (Figure 10b) suggest that this is a glacimarine outwash system. Although we tried to ground-truth this unit at the edge of the sediment lobe, none of the cores managed to sampled this unit. The fact that the coring equipment failed to penetrate the top of the lobe, points to the potential existence of a lag deposit around -80 m water depth and the possible presence of coarser material within the lobe. In the absence of dating and stratigraphic evidence, we tentatively interpret this large sediment lobe as an ice-proximal glacimarine outwash system formed when the ice sheet was retreating between 24 and 18 ka BP. Such systems can form in water depths of several hundred meters (e.g. Simms et al., 2011). As such, while the lobe may be an indicator for the former ice extent, we cannot use its depth as a RSL indicator. However, the possible lag deposit and presence of the seismic surface S4 within the lobe do hint at a basin wide erosional event after ice retreat at a depth around -80 m.

In contrast, in the inner Bay, two cores (BB1 and BB2) did reach the unit in areas where Unit IV infills topographic lows (Figure 8 and 10a). Bio-lithofacies F dominates and the presence of organic material, including *Chenopodium* and *Menyanthes* species, indicate the proximity of a saltmarsh or wetland. The foraminifera assemblages within bio-lithofacies F, particularly those from BB2, appear to show two types of environmental setting. *E. excavatum* and *H. germanica* are both tolerant of large salinity changes (0-35) and brackish environments such as estuaries and lagoons. *H. germanica* is often abundant on tidal flats (e.g., Horton et al., 1999). *E. excavatum* also tends to be abundant in areas that experience high physical disturbance and receive high loads of fresh organic material, including tidal flats or channels (Murray, 1971; Nooijer et al., 2008). However, the dominant *C. obtusa* is a shelf/inner shelf species, living in muddy substrates in deep water (Murray, 2003). Within the Celtic Sea and Western Approaches, a dominance of *C. obtusa* is commonly associated with a number of other species, including *Textularia sagittula*, *Nonionella turgida* and *Cassidulina laevigata* (Murray, 1991); this correlation was not found within our samples. However, *Cassidulina* can also be transported onto intertidal muds (Murray, 2003). Therefore, considering the high abundance of organic material combined with the presence of *E. excavatum* and *H. germanica*, it is possible that this sediment was laid down in shallow intertidal waters The relatively low proportion of broken tests also suggests limited reworking and deposition in a protected environment in the inner Bay.

The laminated nature of bio-lithofacies D, together with the presence of *H. germanica* at the base, suggests a tidally influenced mudflat or a very shallow water estuarine environment (Figures 7 and 10). Foraminifera in bio-lithofacies F are similar to those in bio-lithofacies D, with a prominent presence of estuarine and brackish species. Bio-lithofacies F lacks the clear laminations of facies D and, together with the rare occurrence of bio-lithofacies E (dominated by rounded pebbles and associated with *C. lobatulus* which lives in areas with coarse sediment and/or strong currents (Kristensen and Sejrup, 1996)), is suggestive of occasional episodes of increased sediment influx or higher energy.

Based on these observations, the channels observed on the seismic data in the inner Bay area could have started as meltwater channels draining an outwash plain during the earliest phases of deglaciation, before evolving into tidal channels in a shallow water estuarine setting, transporting organic rich sediments.

Hence, following ice retreat, outwash sediments and estuarine or lagoonal muds infilled depressions, and tidal channels meandered across the outwash plain in the inner Bay during a period of lower than present RSL. Dates for the upper part of this unit (13438 ± 151 a cal BP and 13360 ± 131 a cal BP, Figure 8) show that estuarine conditions were starting to appear in the inner Bay before 13 ka cal BP, prior to the main marine transgression. In coastal plains and lagoonal environments, it is common for initial transgressive sediments to be preserved below the first ravinement surface (S4, see below) (Cattaneo and Steel, 2002).

Unit III: Acoustically this unit can be traced through the basin as U5. It drapes the erosional surface S3 or S4, and is tentatively interpreted as sitting below a wave ravinement surface (S5). It is easily recognisable in the seismic data from its acoustic turbidity with some hyperbola and discontinuous reflectors, often becoming a single reflector at the margins. Core data show that this unit is composed of the clearly laminated lithological unit D (dominant), often with unit F overlying. It contains organic matter and, based on the smell on opening the cores, is rich in hydrogen sulfide. Small amounts of this gas likely produce the turbid acoustic signature with the hyperbolae formed by trapped gas pockets (Bellefleur et al., 2006). Similar gas-related acoustic structures have been detected in neighbouring Dunmanus Bay and have been linked to methane-producing pockmarks (Szpak et al., 2015).

For the cores in the inner Bay, the foraminifera assemblage is similar to the underlying U4, but with an increase in the numbers of fully marine foraminifera. In contrast, the foraminiferal assemblage for the outer Bay core, BB24, is dominated by open marine/inner shelf species. The presence of *C. lobatulus* suggests that this assemblage represents relatively deeper water with potentially strong currents. This mixed assemblage suggests an absence of permanent water column stratification (Scourse et al., 2002). However, the low abundance of *N. turgida* (4%) and *Bulimina* types suggests that sea level was nearing a depth where seasonal stratification could occur. In some of the outer Bay cores, the unit becomes coarser (bio-lithofacies B), but still displays some laminations. Analysis of the foraminifera indicates that this unit records a change from a predominantly estuarine to a mixed estuarine-marine environment, consistent with ongoing transgression.

The reduction in brackish species from Unit IV into Unit III (Figure 8) has been interpreted as an indication for an increase in water depths as RSL rose. In the outer parts of the Bay, the laminated sediments represent an estuarine environment that migrated landwards. In contrast, in the inner Bay the sequence records the change from a muddy organic-rich estuarine lagoonal environment, to a sandier and bioturbated shallow intertidal environment.

The lower boundary (S4) of U5 is interpreted as the tidal ravinement surface. In the outer Bay, this tidal ravinement surface represents the transgressive surface, whilst in the inner Bay, it separates lowstand plus early-transgressive units (Unit IV) from later transgressive units (Unit III, II and I). Unit III represents the transgressive deposits between the tidal ravinement surface at the bottom and a wave ravinement surface at the top. This wave ravinement surface is typically sitting on a sandier unit towards the top of the sequence (bio-lithofacies F). These surfaces are diachronous, and their nature varies depending on the location within the Bay.

Two radiocarbon dates from the overlying units in cores BB18 and BB24 show this unit to be older than 11031 ± 175 a cal BP in the outer Bay. In the inner Bay, on the other hand, a date from the

bottom of Unit III, suggests that this phase of deposition largely occurred post- 11691 ± 286 a cal BP (Figure 8).

Unit II: This unit is predominantly composed of bio-lithofacies D, with some contribution of sandier units B/C. The high concentrations of *Cibicides lobatulus* in the sandy sediments of facies B suggest deposition in a marine, high-energy, well mixed open Bay environment. No micropalaeontological analysis was performed on facies C, but the medium-to-coarse dark grey sand with shell fragments, large broken shells and organic material suggest deposition under high-energy conditions. The varied character of the lithology and the layers of broken shell fragments point towards a transitional unit between estuarine lagoonal, shoreface and inner shelf conditions, under the influence of wave energy and occasional storm deposits in a shallow marine environment. A single radiocarbon date from the bottom of core BB24 indicates that this unit is younger than 10258 ± 152 a cal BP in the offshore region.

Unit I: This unit forms the present seafloor, corresponds to acoustic unit U6b and is composed of bio-lithofacies A or B. In facies B, open marine/inner shelf species dominate the foraminifera assemblage, becoming more abundant up-core, reaching a maximum of 72%. However, the concentration of foraminifera reduces towards the top of the core. This, combined with the high proportion of broken tests (41%), may reflect a high energy and mobile environment that proves difficult for foraminifera to inhabit. In bio-lithofacies A, large assemblage changes are seen between the two investigated inner cores, which is suggestive of an environmentally transitional period. In BB2, the assemblage changes from inner shelf/estuarine dominant at the base of the facies to open marine/inner shelf environment towards the top of this facies. A large reduction in the proportion of *C. obtusa* (4%) suggests that this species is no longer being transported into the muddy estuarine environment. This could be due to the environment changing from an open tidal environment to more restricted environment due to shallowing, stopping *C. obtusa* from reaching this far into the

system. Alternatively, this may indicate a weakening of a high energy regime that previously transported this species into the bay. Uehara et al. (2006) modelled strong tidal currents (1.25 m/s) in the Celtic Sea during early stages of deglaciation, however these declined significantly after 12 ka. This may have had an impact on the mobilisation and transportation of species such as *C. obtusa* into Bantry Bay. In BB6, the appearance of *E. excavatum,* the lack of any other estuarine species and the appearance of *Quinqueloculina sp* and the minor occurrence of *Haynesina depressus* suggest fully marine conditions (Lloyd and Evans, 2002).

Towards the top of the cores a greater influence of open marine species becomes apparent. The association of *Bulimina* with *N. turgida* implies seasonal stratification of the water column, which is depth controlled (Scourse et al., 2002; Scott et al., 2003). Furthermore, *Bulimina* types are infaunal and are associated with fine grained, organic carbon-rich sediments and lowered oxygen levels in the water column (Kristensen and Sejrup, 1996). This, in combination with the decline in estuarine/brackish species, suggests sea levels were rising and water depths increasing.
Both the sedimentology and micro- and macro-fossils therefore suggest an open marine environment in an inner shelf depositional environment.

We plot our ten new radiocarbon dates, together with previously published RSL data from Bantry Bay in Figure 1 and compare them to GIA model predictions of RSL since the LGM. All of our new dates are on monospecific foraminifera that were deposited in environments that existed below the contemporary mean sea level. The dates from BB18 and BB24 (Table 1), from c. 10 - 11 ka cal BP and at water depths of c. 75 to 60 m, lie below the modelled RSL curves at this time by c. 30 m or so, implying their deposition in a subtidal environment. The close agreement between three dates from two cores at the same depth, give confidence in these ages.

The two oldest ages from core BB2 were picked from a laminated, pre-ravinement unit (Unit 4, litho-biofacies F and D (Figure 8)), using monospecific samples of *Elphidium excavatum* and interpreted as having accumulated close to sea level, based on the abundance of *H. germanica* in the same sample interval. The two dates are in close agreement (13.3 – 13.4 ka cal BP) but they plot 10-15 m above the modelled RSL at this time (Figure 1). Studies elsewhere suggest that monospecific foraminifera are susceptible to reworking from older deposits and could therefore be older than the unit in which they accumulated (Heier-Nielson et al., 1995). However, as only 6% of the *E. excavatum* tests are broken, limited reworking is suggested. This suggests that the GIA models require revision to produce greater rebound by, for example a reduction in the viscosity of the lithosphere (e.g. Kuchar and Milne, 2015), and/or thicker ice (e.g. Kuchar et al., 2012). More extensive ice over Bantry Bay is suggested by the new offshore evidence detailed in this paper.

The dates obtained from the transition between *Unit IV* and *Unit III* (i.e. below and above the tidal ravinement surface) from cores BB2 and BB1 confirm the diachroneity of this surface, becoming younger as it reaches shallower parts of the bay (11.7 – 11 ka cal BP). Although these shallow marine dates follow a similar trend, they are again positioned above as the modelled RSL.

6. Discussion

The evidence collected enables us to propose a three-stage model for the evolution of Bantry Bay during the late Quaternary (Figure 11) and compare our findings against the existing GIA models.

The oldest sediments preserved (Unit VI - acoustic unit U2) relate to deposition before the LGM. Although they were not sampled in this investigation, we hypothesise that they are stratigraphically equivalent to the lacustrine silts reported by Stillman (1968). The seismic stratigraphic arrangement of these facies (in topographic lows and topped by a planar erosion surface) suggest a sequence of glacial erosion followed by marine transgression over former lacustrine basins. Similar pockets of pre-LGM sediments have been reported from other southern Irish estuaries (Dowling and Coxon,

2001) and indicate that the last glaciation did not achieve complete excavation of bedrock valleys. The preservation of such pre-glacial sediments is suggestive of areas of frozen-bed (protective) conditions beneath the ice sheet (Hall and Glasser, 2003).

Stage 1 (Figure 11a)*:* The presence of a unit of till (Unit V) throughout the Bay, and associated morainal features offshore, indicates complete filling of the Bay with ice, most likely at the LGM, in agreement with existing interpretations of the LGM ice extent based on onshore data in the area (Ballantyne et al., 2011). Iceberg plough marks offshore are likely derived from locally-sourced calving margins.

The ice sheet deposited an ice-proximal glacimarine outwash system (Figure 11a), now preserved as a large sediment lobe at the mouth of Bantry Bay.

Although some weak foresets are detected on the seismic data, no topsets are seen, suggesting that this was a subaqueous fan with no subaerial component. This suggests that sea-level was likely higher than the top of this outwash fan (ca. 80 m water depth) during the early phase of deglaciation, post 24 ka BP, before falling to a lowstand around 20 ka BP as predicted by the GIA models. We interpret the position of the former ice-proximal glacimarine outwash system at the mouth of the bay as the limit of the ice margin extent in Bantry Bay. A series of submarine moraines, located to the west of the outwash system and now buried a few meters below the present seabed, may be associated with the ice retreat phase (Figure 9).

Stage 2 (Figure 11b)*:* These moraines were subsequently partially buried and reworked by waves and strong tidal currents after ice retreat. In order for this reworking to take place, sea level must have been low enough for tidal and wave processes to have a significant impact on the seabed.

The reworking produced a lowstand shoreline complex comprising shoreface ridges (the long linear ridges that dominate the modern seabed in water depths between 80 m and 130 m (Figure 11b)), a scarp cut into outwash sediments between 76 and 94 m (the scarp on the northern edge of

sediment lobe (Figure 4 C3)), and the erosional surface (S4) on top of the lobe which has been traced to a maximum depth of 84 m (Figure 10b). The development of these features points to a significant period of quasi stable sea level, which we interpret to have occurred at a depth of around 80 m water depth. According to the GIA models (Figure 1), such a lowstand period preceded MWP-1A and was prevalent for at least 5000 years (ca. 20 – 14.6 ka BP).

Shallower ridges sitting on top of the proposed sediment lobe (Figure 4 C3) and on top of the tidal ravinement surface, suggest they formed when RSL was already rising, which, as suggested by Brooks et al. (2008), occurred after 14.6 ka BP.

During and after ice-retreat, topographic lows on the exposed till surface became infilled with outwash sediments and lagoonal muds (stratigraphic Unit IV inshore) in the inner part of the Bay, fed by outwash channels.

Preservation of coastal features from further wave reworking on this high energy coast implies rapid sea-level rise, such as that attributed to meltwater pulses (e.g. Green et al., 2014).

Stage 3 (Figure 11c)*:* As RSL rose rapidly after 14.6 ka BP, the sea transgressed and the coastline retreated landwards, the sediment lobe was fully inundated and an estuarine system was firmly established, whilst the channels became tidal (Figure 11c), as evidence by the high organic content of the sediments and the presence of *E. excavatum* and *H. germanica*. This is the point at which the tidal ravinement surface (S4) migrated landwards.

On the seismic data, the main ravinement surface (S4) is present on top of the sediment lobe on the landward side of the long tidal ridges, where it represents the transgressive surface, and in the inner Bay, where it represents the tidal ravinement surface above the transgressive surface; it clearly pinches out towards the side of the basin (Figure 12a). This surface marks a clear increase in water depth.

The depth profile of S4 (Figure 12c), which is based solely on the seismic data, reveals S4 to be very flat at the Bay mouth, at a depth of around 78 m. Where the Bay starts to narrow, between the tip

of Sheep's Head and Bere Island, the profile changes to a fairly linear, low angle slope (c. 0.07°) which can be traced all the way to the head of the Bay. A comparison between this profile and the modelled sea-level curve (Figure 12d) shows a very similar shape: a flat RSL around -78 m during and just after the ice retreat, followed by a rapid sea-level rise after 14.6 ka BP (melt-water pulse 1A). The transition from a flat to a low angle profile for S4 may reflect an increase in the rate of RSL during the Late Glacial, potentially at or about the timing of MWP-1A. Our radiocarbon dates from the inner Bay suggest that the main ravinement surface (S4) is diachronous, but was initiated sometime after c. 13 ka BP (Figure 8) in the inner part. As we note above, the pair of dates from core BB2 (Unit IV ca. 13.4 k cal BP at around -41 m) suggest that RSL was higher than predicted by existing GIA models, shortly after MWP-1A.

Data from the far-field (Tahiti) give approximate rates of RSL rise during MWP-1A of c. >40 mm yr^{-1} between 14.6 and 14.31 ka BP (Deschamps et al., 2012), which is of the same order as suggested by our dates: an approximate rise of 30 mm yr^{-1} between 14.6 and 13.4 ka BP. Recent results (Liu et al., in review) suggest that the global mean amplitude of MWP-1A was in the range of 11-14 m which, incorporated in the local GIA models (taking into account ice unloading), would result in an RSL rise of no more than 10-20 m.

An abrupt rise in RSL, whether it be in the order of 10 to 20 m or up to 40 m would cause a rapid landward shift of the coastline over a period of about a thousand years (Figure 12e&d; reconstruction assumes the transgressive surface is buried beneath an average of 3 m of sediments). Such abrupt RSL rise, linked to MWP-1A, would be expected to have caused shoreline overstepping, and preservation of the former coastal sediments (Green et al., 2013; 2014). Although this appears to be the case in Bantry Bay (preservation of lowstand shoreline complex), it is not evident in the long profile of the ravinement surface. Similarly, the ravinement surface does not reflect the period of slower sea-level rise ('slowstand') predicted by the GIA models between 11 – 13.5 ka cal BP (Figure 1). However, the radiocarbon dates do suggest a higher RSL than predicted by the models between 13.4 and 11.0 ka BP (Figure 12d). They are also suggestive of a stillstand. This dichotomy

cannot be resolved with existing data: more systematic sampling at the critical depths predicted by the GIA models (between ca. -55 and -75 m) is required.

The basal transgressive unit (U5, stratigraphic unit III) overlying the ravinement surface is thickest just offshore of the inflection point seen on the transgressive surface profile, where it can reach a thickness of 6 m (Figure 12b). The accumulation of sediments in this area is most likely the result of a RSL stillstand after the LGM (pre-14.6 ka cal BP; Figure 12e). Although this unit was not cored at this location, the sediments recovered further offshore suggest that these deposits are mainly sandy. Moving into the bay, this unit rarely reaches 3 m thickness and is younger than 13 ka cal BP. Inshore, the sediments of stratigraphic unit III suggest a 'mixflat' (mixed tidal flat, as defined by Traini et al. (2013)). The organic matter and smell of gas in the cores, explains the turbid acoustic signature. It could be derived from terrestrial vegetation, growing at the edge of the basin. By this point, the tidal channels would have been filled and an estuarine system would have been well established at the mouth of the bay. Finally, these tidal and estuarine sediments are capped by a wave ravinement surface (S5), which potentially created a hiatus with the overlying fully marine sediments (stratigraphic units II and I).

7. Conclusions

This paper presents the first offshore data relating to the Late Quaternary history of Bantry Bay, Ireland, including its drowning after the LGM. Our main conclusions are:

1. The oldest sediments preserved record a phase of marine transgression some time before the LGM. These sediments are confined to topographic lows and are overlain by a glacial diamict formed as ice advanced. Iceberg scours testify to calving from a marine-based ice margin, which extended seaward of the contemporary Bay pre-18 ka BP. A significant sand body at the mouth of the Bay has been interpreted as a glacimarine outwash system. Parts of the glacial diamict were eroded and

redeposited as a thin sequence of sediment, with channels in the inner Bay indicating a lower than present sea level. In the outer Bay, an erosional surface on the top of the sand body, and a scarp on its north-western side, have been interpreted as evidence for a RSL lowstand around -80 m shortly after the LGM.

2. Linear ridges in the outer part of the Bay are interpreted as having formed under stronger than present tidal currents, during a period of stable RSL between 20 and 14.6 ka BP.

3. At or shortly after ~14 ka BP, RSL rise led to the development of an extensive transgressive system tract and the formation of an estuarine depositional environment across much of the central and inner parts of Bantry Bay. Radiocarbon dates obtained below the tidal ravinement surface indicate that, in the inner Bay, the initial estuarine influence started before 13 ka cal BP. This diachronous surface can be traced on the seismic data from a depth of -78 m in the offshore region, where the surface is flat, into the inshore bay, where it shows a gentle slope. In the inner Bay, laminated organic-rich sediments together with the presence of the foraminifera *Haynesina germanica* suggest a tidally influenced mudflat or a very shallow water estuarine environment at the time of transgression, becoming open marine towards the top.

4. The litho- and seismostratigraphic data resolve broad-scale RSL rise and estuary transgression. However, our dates do not fully agree with the GIA models for the site, as they suggest a higher sea-level than predicted between 11-13.5 ka BP. Although these radiocarbon dates display a similar trend as the GIA models, there is no clear evidence for MWP-1A or such a subsequent 'slowstand' on the seismic data.

5. This study is the first stage in the development of a more regional post-LGM seismo-stratigraphic model for the offshore region of Ireland. These findings form an important basis for the

improvement of regional GIA models and our understanding of the impact of global events (e.g. MWP-1A) on RSL in this region. A mismatch between our radiocarbon dates, together with the depth of the ravinement surface traced from the seismic data, are suggestive of issues with the current Earth model and/or ice sheet extent or thickness used by the GIA models. Better constrained GIA models will ultimately lead to more accurate palaeogeographic reconstructions of the Celtic Sea region throughout the last deglacial cycle.

Acknowledgements

This study is part of the NERC funded project NE/H024301/1, 'Late Glacial Sea Level Minima'. Thanks to Fabio Sacchetti, INFOMAR, MI, GSI, Connor McCarron, Will Evans, Andy Green, Master and Crew of *RV Celtic Explorer* and *RV Celtic Voyager*, who all helped with the data collection. We thank Dr Xiaomei Xu at the Keck C cycle AMS Lab, University of California, for analysing the small radiocarbon samples. IHS provided Kingdom Suite to the School of Environmental Sciences at the Ulster University under the University Gift Program. This work was supported by the NERC Radiocarbon Facility NRCF010001 (allocation number 1683.1112). Finally, we would like to thank two anonymous reviewers for their detailed comments, which have helped to improve this manuscript.

REFERENCES

Ballantyne, C.K., McCarroll, D., Stone, J.O., 2006. Vertical dimensions and age of the Wicklow Mountains ice dome, Eastern Ireland, and implications for the extent of the last Irish Ice Sheet. Quaternary Science Reviews 25, 2048-2058.

Ballantyne, C.K., McCarroll, D., Stone, J.O., 2011. Periglacial trimlines and the extent of the Kerry-Cork Ice Cap, SW Ireland. Quaternary Science Reviews 30, 3834-3845.

Barnhardt, W.A., Belknap, D.F., Kelley, J.T., 1997. Stratigraphic evolution of the inner continental shelf in response to late Quaternary relative sea-level change, northwestern Gulf of Maine. Geological Society of America Bulletin 109, 612-630.

Belderson, R.H., Kenyon, N.H., Wilson, J.B., 1973. Iceberg Plough Marks in the Northeast Atlantic. Palaeogeography, Palaeoclimatology, Palaeoecology 13, 215-224.

Bellec, V., Wilson, M., Bøe, R., Rise, L., Thorsnes, T., Buhl-Mortensen, L., Buhl-Mortensen, P., 2008. Bottom currents interpreted from iceberg ploughmarks revealed by multibeam data at Tromsøflaket, Barents Sea. Mar. Geol. 249, 257-270.Bellefleur, G., Duchesne, M.J., Hunter, J., Long, B.F., Lavoie, D., 2006. Comparison of single- and multichannel high-resolution seismic data for shallow stratigraphy mapping in St. Lawrence River estuary, Quebec, in: Canada, G.S.o. (Ed.). National Resource Canada, p. 10.

Blake, C.B., 2005. Use of maerl as a biogenic archive. Unpublished PhD thesis. Biological Sciences, Queen's University Belfast, Belfast.

Bradley, S.L., Milne, G.A., Shennan, I., Edwards, R., 2011. An improved Glacial Isostatic Adjustment model for the British Isles. Journal of Quaternary Science 26, 541-552.

Brooks, A.J., Bradley, S.L., Edwards, R.J., Goodwyn, N., 2011. The palaeogeography of Northwest Europe during the last 20,000 years. Journal of Maps, 573-587.

Brooks, A.J., Bradley, S.L., Edwards, R.J., Milne, G.A., Horton, B., Shennan, I., 2008. Postglacial relative sea-level observations from Ireland and their role in glacial rebound modelling. Journal of Quaternary Science 23, 175-192.

Brooks, A.J., Edwards, R.J., 2006. The development of a sea-level database for Ireland. Irish Journal of Earth Sciences 24, 13-27.

Butler, P.G., Scourse, J.D., Richardson, C.A., Wanamaker, A.D., Bryant, C.L., Bennell, J.D., 2009. Continuous marine radiocarbon reservoir calibration and the C-13 Suess effect in the Irish Sea: Results from the first multi-centennial shell-based marine master chronology. Earth and Planetary Science Letters 279, 230-241.

Cattaneo, A., Steel, R.J., 2003. Transgressive deposits: a review of their variability. Earth-Science Reviews 62, 187-228.

Clark, C.D., Hughes, A.L.C., Greenwood, S.L., Jordan, C., Sejrup, H.P., 2012. Pattern and timing of retreat of the last British-Irish Ice Sheet. Quaternary Science Reviews 44, 112-146.

Clark, P.U., Dyke, A.S., Shakun, J.D., Carlson, A.E., Clark, J., Wohlfarth, B., Mitrovica, J.X., Hostetler, S.W., McCabe, A.M., 2009. The Last Glacial Maximum. Science 325, 710-714.

Deschamps, P., Durand, N., Bard, E., Hamelin, B., Carmoin, G., Thomas, A.L., Henderson, G.M., Okuno, J., Yokoyama, Y., 2012. Ice-sheet collapse and sea-level rise at the Bølling warming 14,600 years ago. Nature 483 (7391), 559-564.

Dowdeswell, J.A., Ottesen, D., Evans, J., Ó Cofaigh, C., Anderson, J.B., 2008. Submarine glacial landforms and rates of ice-stream collapse. Geology 36, 819-822.

Dowling, L.A., Coxon, P., 2001. Current understanding of Pleistocene temperate stages in Ireland. Quaternary Science Reviews 20, 1631-1642.

Dunlop, P., Shannon, R., McCabe, M., Quinn, R., Doyle, E., 2010. Marine geophysical evidence for ice sheet extension and recession on the Malin Shelf: New evidence for the western limits of the British Irish Ice Sheet. Marine Geology 276, 86-99.

Edwards, A., Jones, K., Graham, J.M., Griffiths, C.R., MacDougall, N., Patching, J., Richard, J.M., Raine, R., 1996. Transient coastal upwelling and water circulation in Bantry Bay, a ria on the south-west coast of Ireland. Estuarine Coastal and Shelf Science 42, 213-230.

Green, A.N., Cooper, J.A.G., Leuci, R., Thackeray, Z., 2013. Formation and preservation of an overstepped segmented lagoon complex on a high-energy continental shelf. Sedimentology 60, 1755-1768.

Green, A.N, Cooper, J.A.G. and Saltzmann, L. 2014. Geomorphic and stratigraphic signals of postglacial meltwater pulses on continental shelves. Geology, 42, 151-154.

Hall, A. M., Glasser, F., 2003. Reconstructing former glacial basal thermal regimes in a landscape of selective linear erosion: Glen Avon, Cairngorm Mountains, Scotland. Boreas 32, 191-207.

Harkness, D.D., 1983. The extent of the natural 14C deficiency in the coastal environment of the United Kingdom. Journal of the European Study Group on Physical, Chemical and Mathematical Techniques Applied to Archaeology PACT 8, 351-364.

Haynes, J.R., 1973. Cardigan Bay recent foraminifera: cruise of the R.V. Anthur, 1962-1964., The Bulletin of the British Museum (Natural History) Zoology supplement, p. 245.

Heier-Nielsen, S., , Conradsen, K., Heinemeier, J., Knudsen, K.L., Nielsen, H.L., Rud, N., Sveinbjörnsdóttir, Á.E., 1995. Radiocarbon dating of shells and foraminifera from the Skagen core, Denmark: evidence of reworking. Radiocarbon., 37(2), 119-130.

Hiemstra, J.F., Evans, D.J.A., Scourse, J.D., McCarroll, D., Furze, M.F.A., Rhodes, E., 2006. New evidence for a grounded Irish Sea glaciation of the Isles of Scilly, UK. Quaternary Science Reviews 25, 299-309.

Hill, J.C., Gayes, P.T., Driscoll, N.W., Johnstone, E.A., Sedberry, G.R., 2008. Iceberg scours along the southern U.S. Atlantic margin. Geology 36, 447-450.Horton, B.P., Edwards, R.J., Lloyd, J.M., 1999. UK intertidal foraminiferal distributions: implications for sea-level studies. Marine Micropaleontology 36, 205-223.

Kristensen, D.K., Sejrup, H.P., 1996. Modern benthic foraminiferal biofacies across the northern North Sea. Sarsia 81, 97-106.

Kuchar, J., Milne, G., Hubbard, A., Patton, H., Bradley, S., Shennan, I., Edwards, R., 2012. Evaluation of a numerical model of the British-Irish ice sheet using relative sea-level data: implications for the interpretation of trimline observations. Journal of Quaternary Science 27, 597-605.

Kuchar, J., Milne, G.A., 2015. The influence of viscosity structure in the lithosphere on predictions from models of glacial isostatic adjustment. Journal of Geodynamics 86, 1-9.Liu, Z.X., Berne, S., Saito, Y., Yu, H., Trentesaux, A., Uehara, K., Yin, P., Liu, P., Li, C.X., Hu, G.H., Wang, X.Q., 2007. Internal architecture and mobility of tidal sand ridges in the East China Sea. Continental Shelf Research 27, 1820-1834.

Liu, J., Milne, G.A., Kopp R.E., Clark P.U., Shennan, I. (in review). Sea-level constraints on the source distribution and amplitude of Meltwater Pulse 1A. Nature Geoscience.

Lønne, I., 1995. Sedimentary facies and depositional architecture of ice-contact glaciomarine systems. Sedimentary Geology 98, 13-43.

McCarroll, D., Stone, J.O., Ballantyne, C.K., Scourse, J.D., Fifield, L.K., Evans, D.J.A., Hiemstra, J.F., 2010. Exposure-age constraints on the extent, timing and rate of retreat of the last Irish Sea ice stream. Quaternary Science Reviews 29, 1844-1852.

Murray, J.W., 1971. An atlas of British recent foraminids. Heinemann Educational Books, London.

Murray, J.W., 1979. British nearshore foraminiferids; key and notes for the identification of species. Academic Press, London.

Murray, J.W., 2003. An illustrated guide to the benthic foraminifera of the Hebridean Shelf, west of Scotland, with notes on their mode of life. Palaeontologia Electronica 5, 1-31.

Nooijer, L.J., Duijnstee, I.A.P., Bergman, M.J.N., van der Zwaan, G.J., 2008. The ecology of benthic foraminifera across the Frisian Front, southern North Sea. Estuarine, Coastal and Shelf Science 78, 715-726.

Ó Cofaigh, C., Telfer, M.W., Bailey, R.M., Evans, D.J.A., 2012a. Late Pleistocene chronostratigraphy and ice sheet limits, southern Ireland. Quaternary Science Reviews 44, 160-179.

Ó Cofaigh, C., Dunlop, P., Benetti, S., 2012b. Marine geophysical evidence for Late Pleistocene ice sheet extent and recession off northwest Ireland. Quaternary Science Reviews 44, 147-159.

Pantin, H.M., 1977. Quaternary sediments of the northern Irish Sea, in: Kidson, C., Tooley, M.J. (Eds.), The Quaternary History of the Irish Sea. Seel House Press, Liverpool, pp. 27–54.

Pracht, M., Sleeman, A.G., 2002. Geology of West Cork, in: Ireland, G.S.o. (Ed.). Department of Public Enterprise, p. 79.

Queen's University Belfast (QUB) ^{14}Chrono Centre. Marine Reservoir Correction database. Available from: http://calib.qub.ac.uk/marine/. Last accessed: 02/12/2013.

Reimer, P.J., , Bard, E., Bayliss, A., Beck, J.W., Blackwell, P.G., Ramsey, C.B., Buck, C.E., Cheng, H., Edwards, R.L., Friedrich, M., Grootes, P.M., Guilderson, T.P., Haflidason, H., Hajdas, I., Hatté, C., Heaton, T.J., Hoffmann, D.L., Hogg, A.G., Hughen, K.A., Kaiser, K.F., Kromer, B., McCormac, F.G., Manning, S.W., Nui, M., Reimer, R.W., Richards, D.A., Scott, E.M., Southon, J.R., Staff, R.A., Turney, C.S.M., van der Plicht, J., 2013. Intcal13 and Marine13 Radiocarbon Age Calibration Curves, 0-50,000 Years Cal Bp. Radiocarbon 55, 1869-1887.

Roycroft, D., Kelly, T.C., Lewis, L.J., 2004. Birds, seals and the suspension culture of mussels in Bantry Bay, a non-seaduck area in Southwest Ireland. Estuarine Coastal and Shelf Science 61, 703-712.

Sacchetti, F., Benetti, S., Ó Cofaigh, C., Georgiopoulou, A., 2012. Geophysical evidence of deep-keeled icebergs on the Rockall Bank, Northeast Atlantic Ocean. Geomorphology 159, 63-72.

Scott, G.A., Scourse, J.D., Austin, W.E.N., 2003. The distribution of benthic foraminifera in the Celtic Sea: The significance of seasonal stratification. Journal of Foraminiferal Research, 33, 32-61

Scourse, J.D., Austin, W.E.N., Long, B.T., Assinder, D.J. ,Huws, D., 2002. Holocene evolution of season stratification in the Celtic Sea: refined age model, mixing depths and foraminiferal stratigraphy. Marine Geology, 191, 119-145.

Scourse, J.D., Haapaniemi, A.I., Colmenero-Hidalgo, E., Peck, V.L., Hall, I.R., Austin, W.E.N., Knutz, P.C., Zahn, R., 2009a. Growth, dynamics and deglaciation of the last British-Irish ice sheet: the deep-sea ice-rafted detritus record. Quaternary Science Reviews 28, 3066-3084.

Scourse, J., Uehara, K., Wainwright, A., 2009b. Celtic Sea linear tidal sand ridges, the Irish Sea Ice Stream and the Fleuve Manche: Palaeotidal modelling of a transitional passive margin depositional system. Marine Geology 259, 102-111.

Sejrup, H.P., Haflidason, H., Aarseth, I., King, E., Forsberg, C.F., Long, D., Rokoengen, K., 1994. Late Weichselian Glaciation History of the Northern North-Sea. Boreas 23, 1-13.

Sejrup, H.P., Hjelstuen, B.O., Dahlgren, K.I.T., Haflidason, H., Kuijpers, A., Nygard, A., Praeg, D., Stoker, M.S., Vorren, T.O., 2005. Pleistocene glacial history of the NW European continental margin. Marine and Petroleum Geology 22, 1111-1129.

Stewart, H., Bradwell, T., 2014. The use of multibeam backscatter intensity data as a tool for mapping glacial deposits in the Central North Sea, UK Geophysical Research Abstracts 16, EGU2014-abstract number 16616.Stillman, C.J., 1968. The post glacial change in sea level in south-western Ireland: new evidence from fresh-water deposits on the floor of Bantry Bay. Scientific Proceedings of the Royal Dublin Society A3, 125-127.

Traini, C., Menier, D., Proust, J.N., Sorrel, P., 2013. Transgressive systems tract of a ria-type estuary: The Late Holocene Vilaine River drowned valley (France). Marine Geology 337, 140-155.

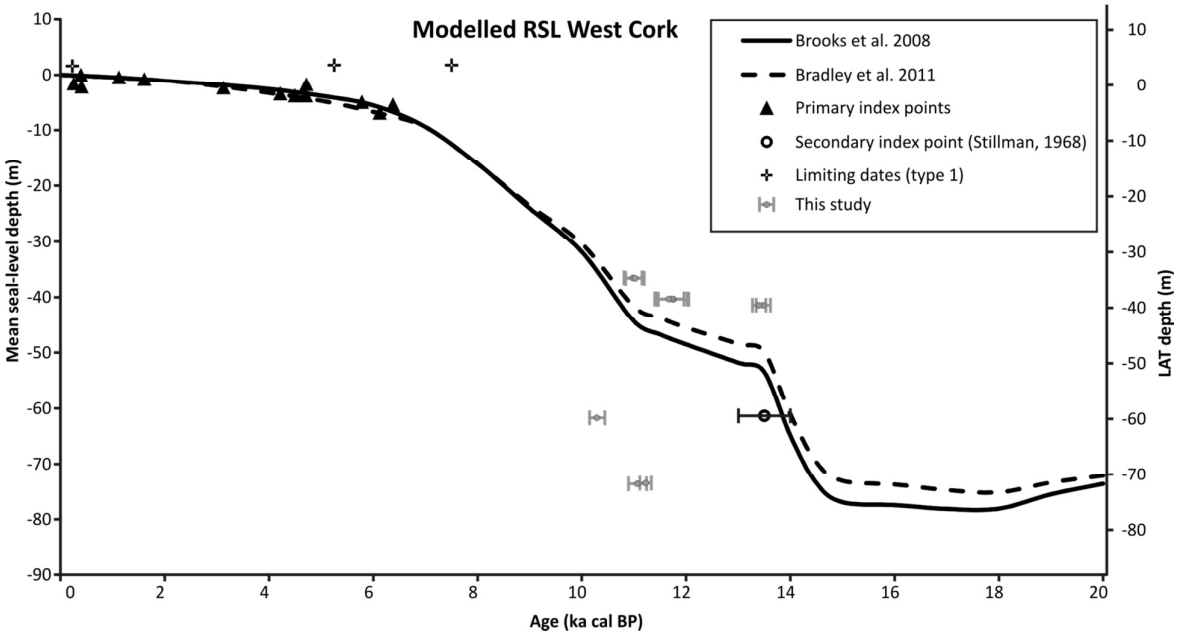

Figure 1. GIA model for West Cork according to Brooks et al. (2008) and Bradley et al. (2011); for a definition of limiting dates, primary and secondary index points, the reader is referred to Brooks et al. (2008).

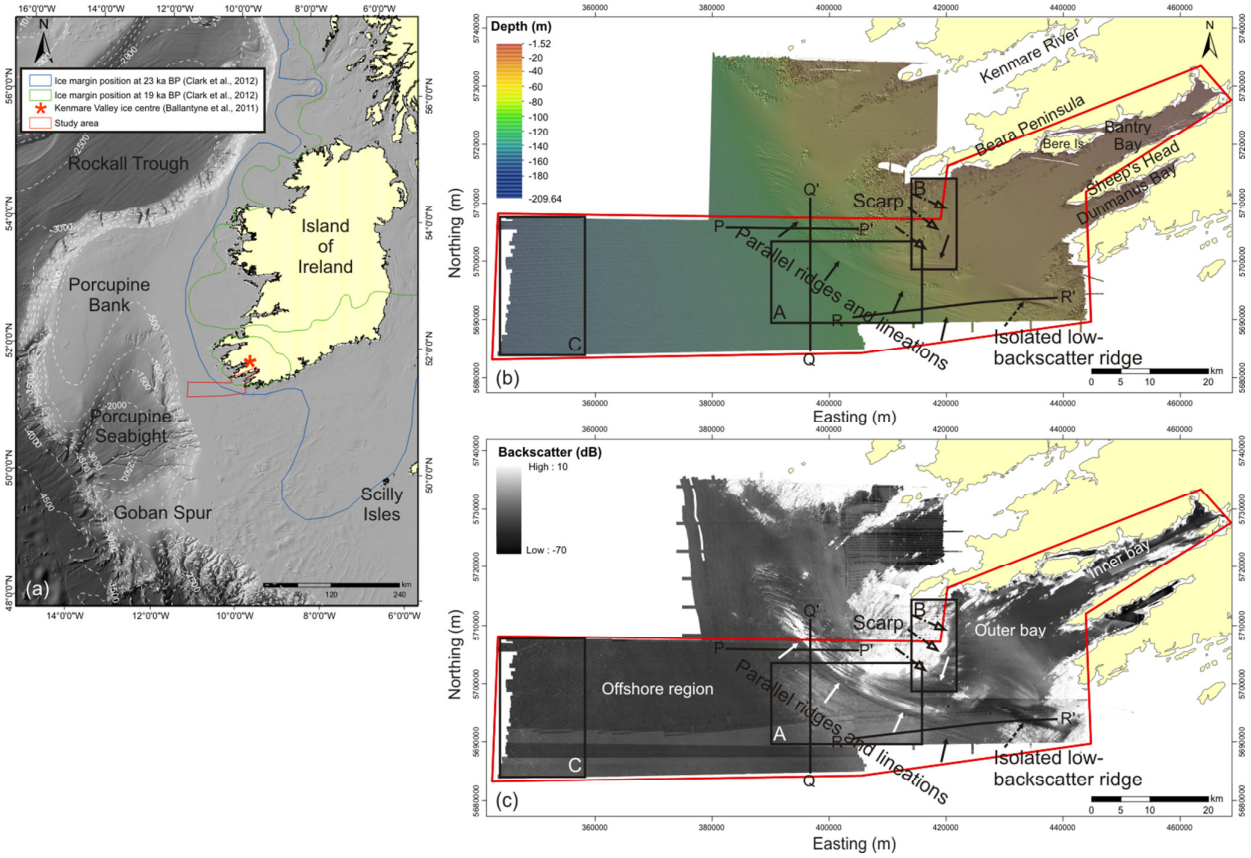

Figure 2. (a) Regional location map of the study area (red box), showing the position of the ice sheet margin at the LGM and before the final phase of ice retreat from Bantry Bay (from Clark et al., 2012); red asterisk shows location of the Kenmare ice centre (Ballantyne et al., 2011) – background bathymetry from EMODnet (http://www.emodnet-hydrography.eu/); (b) detailed Bathymetric data and (c) backscatter data of the study area. Boxes A, B and C refer to figure 4; Profiles PP', QQ' and RR' refer to Figure 10; Full arrows: long parallel ridges and lineations; broken arrow: tall isolated, low-backscatter ridge; dotted-broken arrow: scarp.

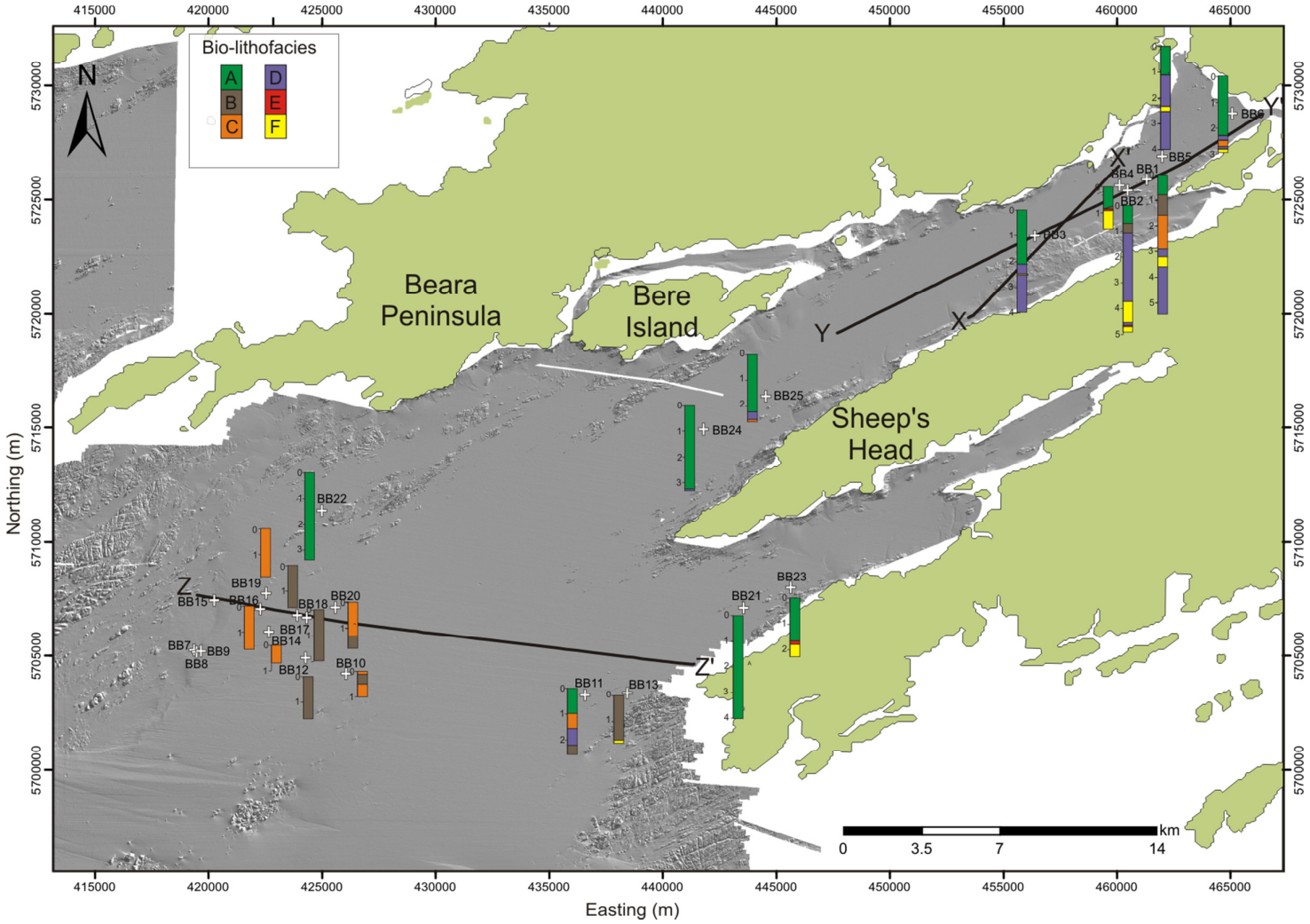

Figure 3. Location and lithology of vibrocore sites. Profiles XX', YY' and ZZ' refer to seismic lines shown in figures 6 and 9.

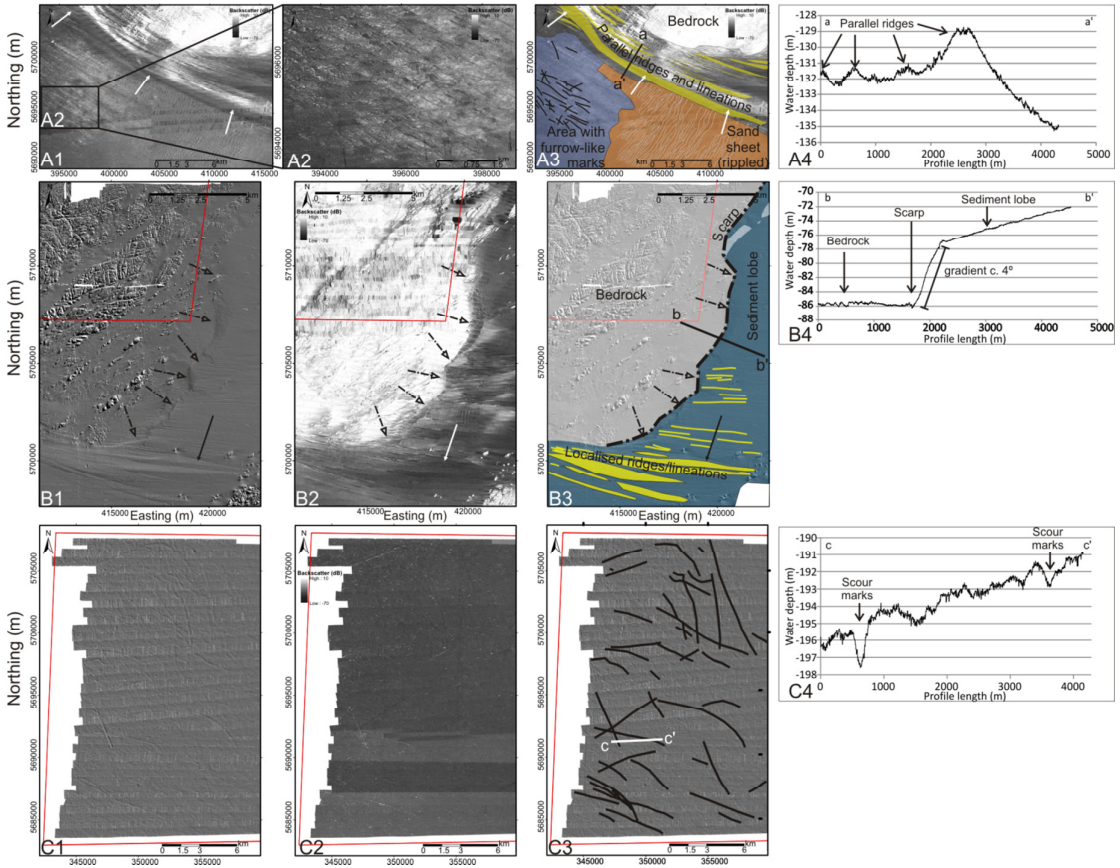

Figure 4. (A1) Backscatter data, with (A2) showing more detail, and (A3) mapping of the (iceberg) scour features and the long parallel ridges imaged at the mouth of the Bay; (A4) shows a profile through these ridges. (B1) Bathymetric and (B2) backscatter data of the scarp, with (B3) showing an interpretation of the detected features and (B4) a depth profile of the scarp. (C1) Bathymetric and (C2) backscatter data, and (C3) mapping of the (iceberg) scour marks in the deeper parts of the study area, with (C4) showing a depth profile through these scour marks. Full arrows: long parallel ridges and lineations; broken arrow: tall isolated, low-backscatter ridge; dotted-broken arrow: scarp. For location of these boxes, see figure 2.

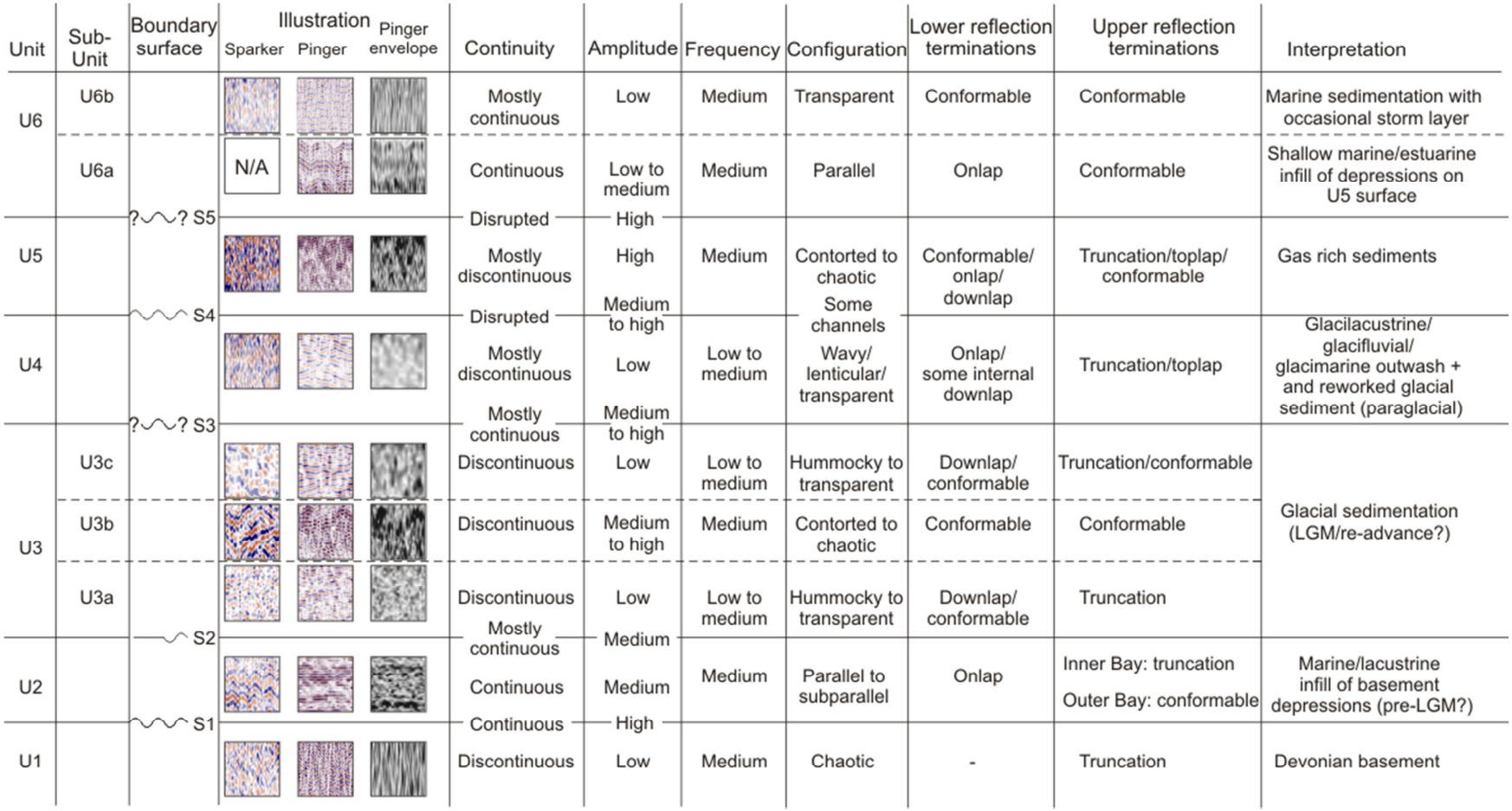

Figure 5. Summary of the nature of the seismo-stratigraphic units and associated bounding surfaces.

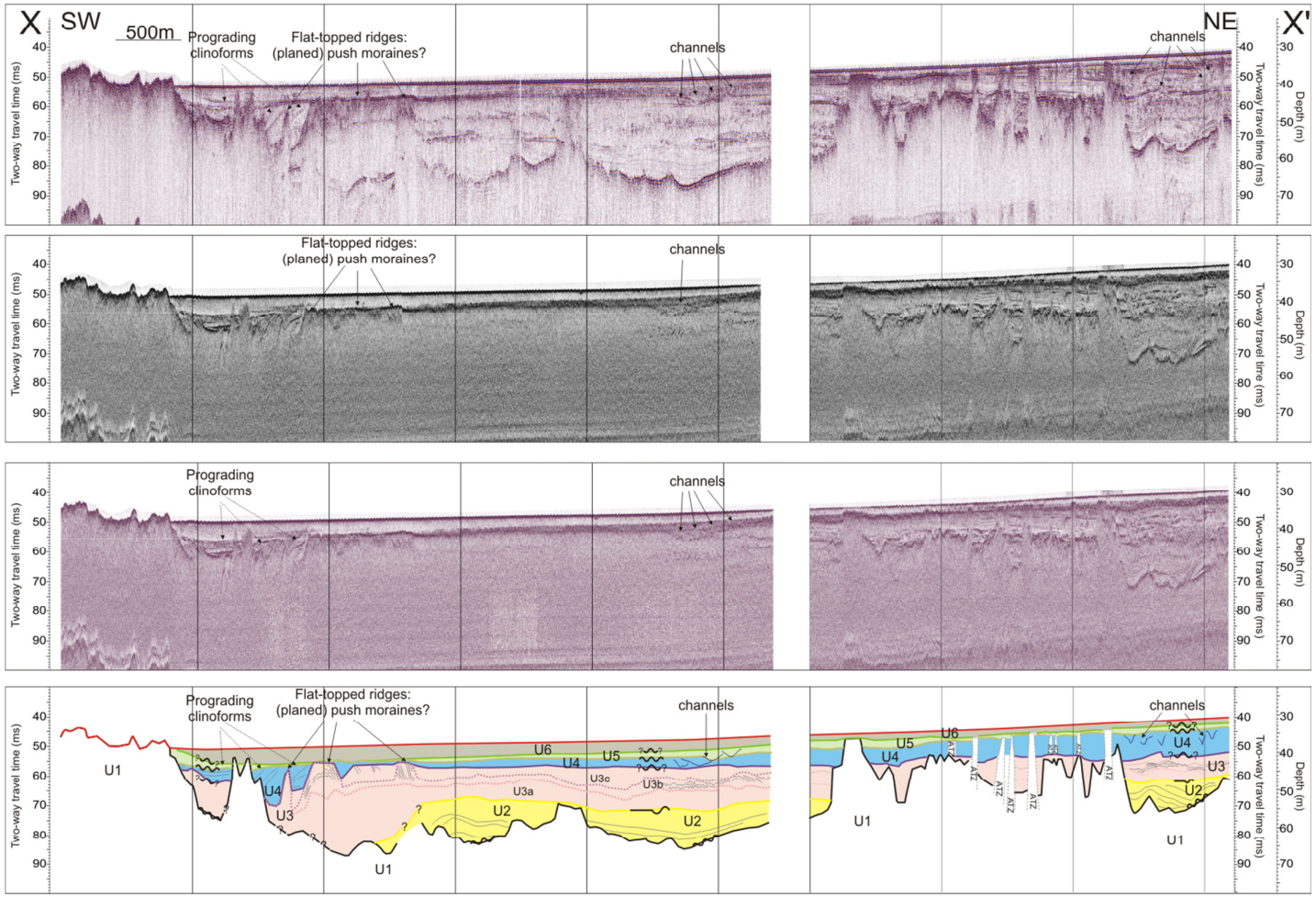

Figure 6. Sparker (top) and pinger (with envelope: middle; without envelope: bottom) line with the seismo-stratigraphic interpretation. For the location of the line, see Figure 3. ATZ = acoustic turbidity zone.

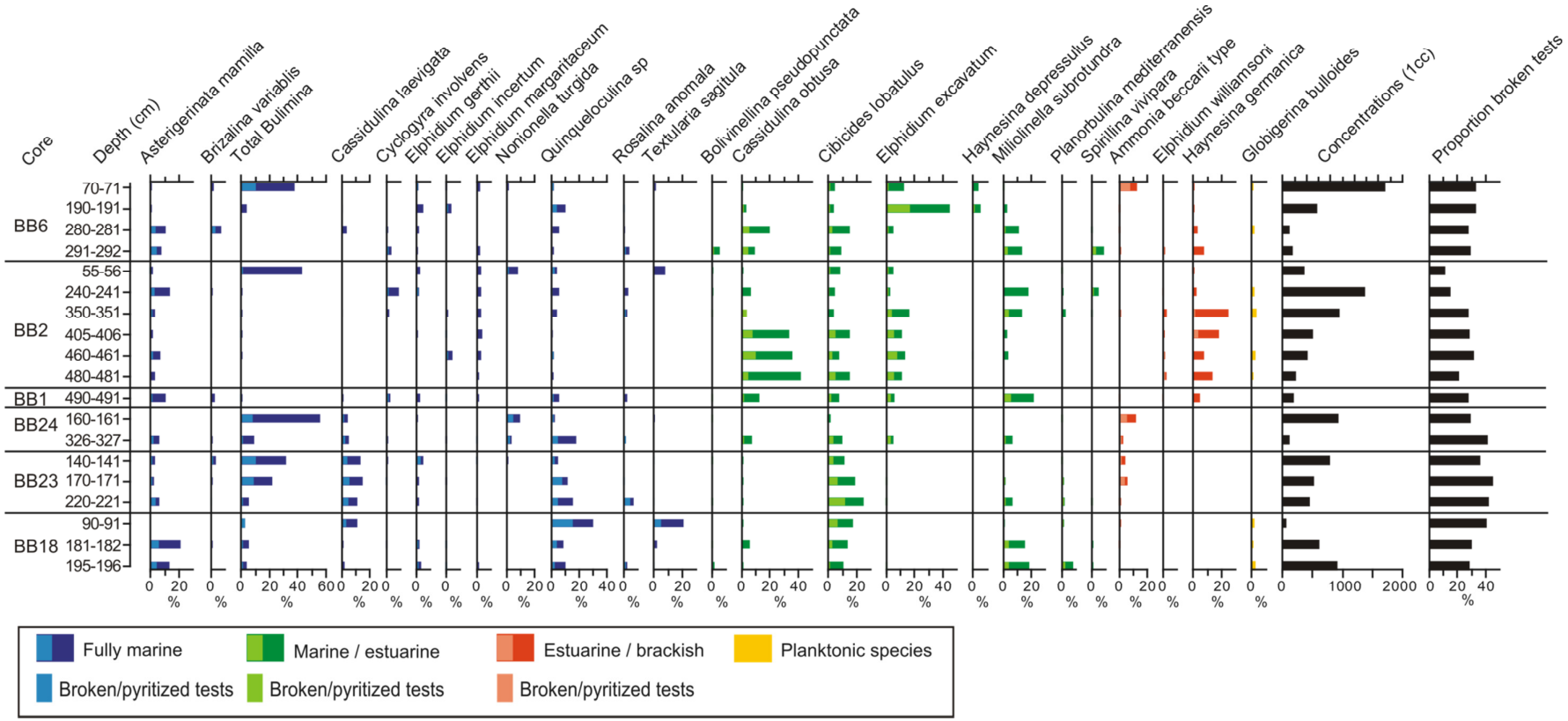

Figure 7. Analysis of the most abundant foraminifera. The lighter coloured portion of each bar plot shows the fraction of broken or pyritized tests versus unbroken (darker colour) tests. For a list of all examined species, see the table and figure in Appendix 1 2 and 23.

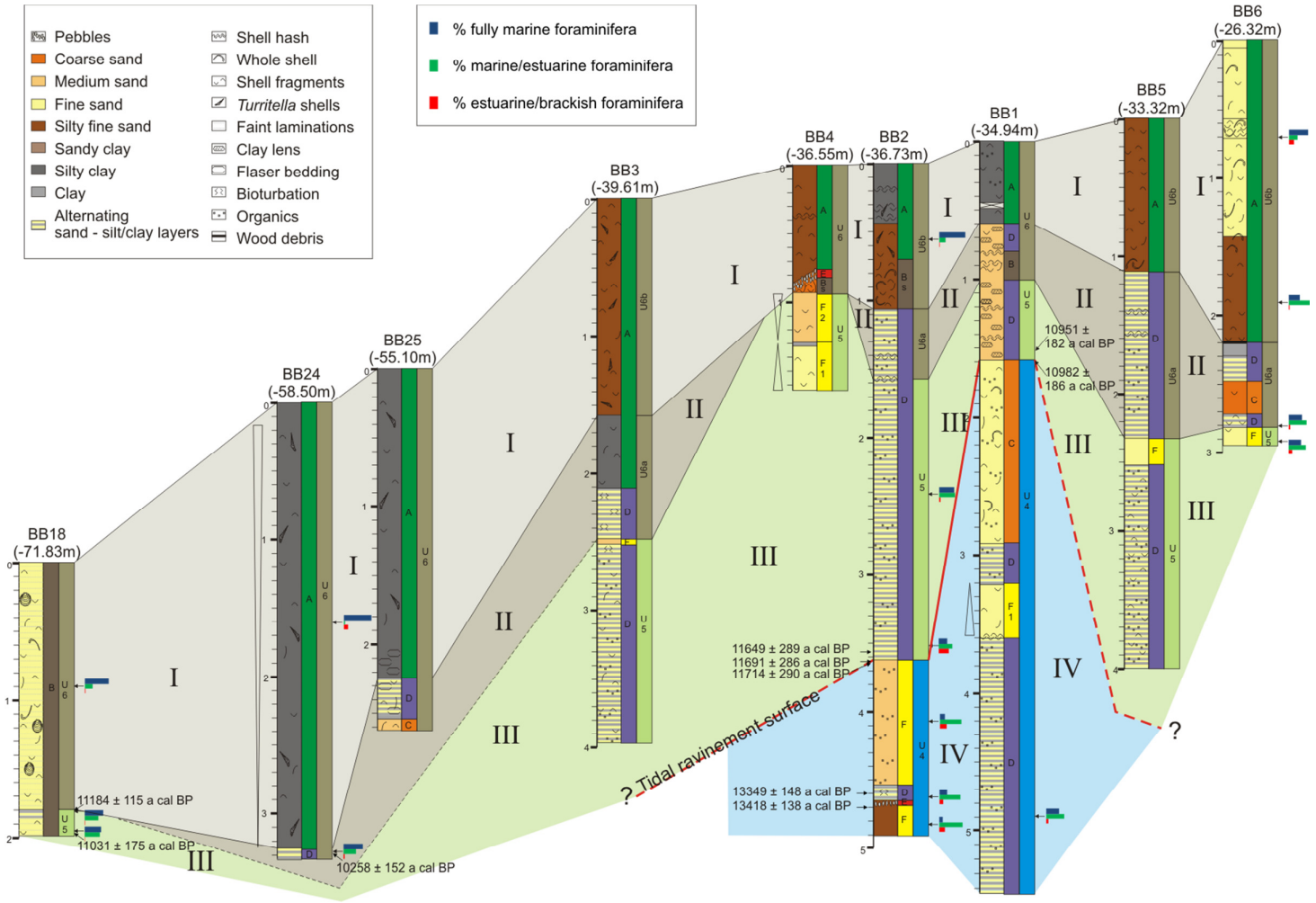

Figure 8. Correlation of cores through the bay showing the stratigraphic relationship between seismo-, litho- and bio-stratigraphic data; water depths are to MSL.

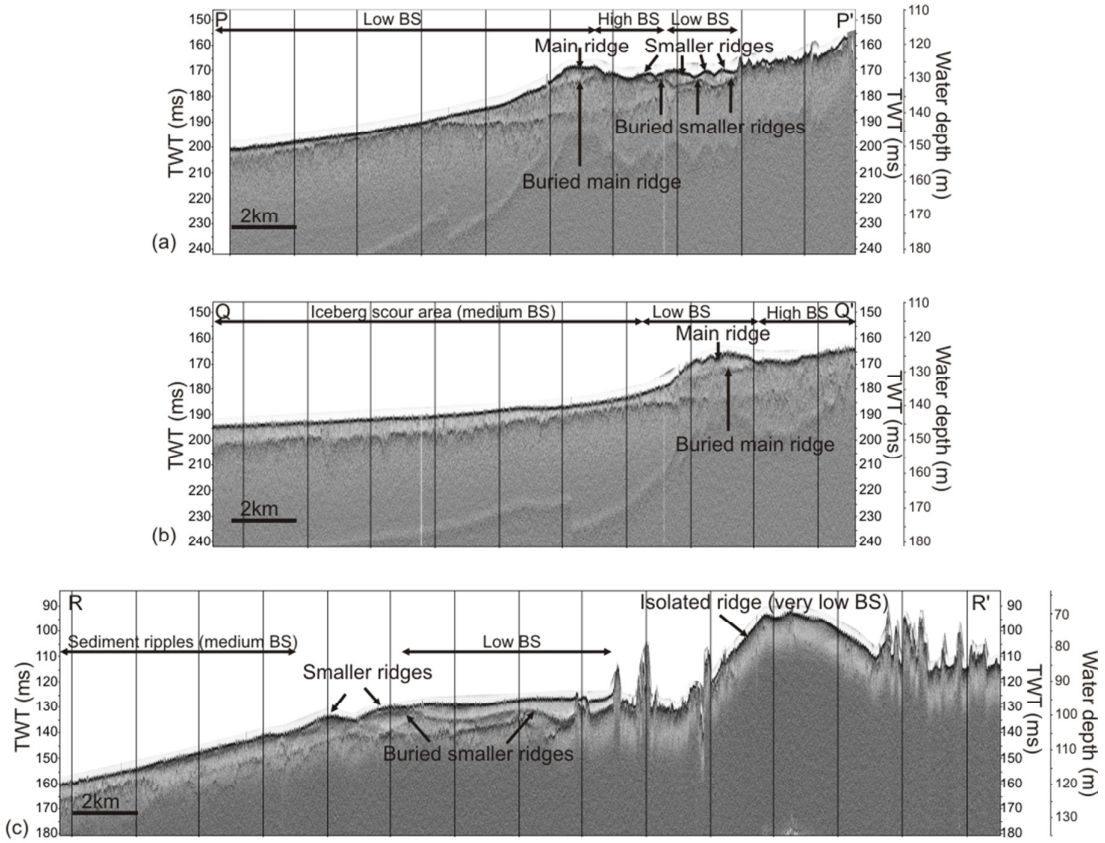

Figure 9.Pinger profiles through some of the ridges found at the mouth of the Bay, with the position of the pinger profiles shown in Figure 2. BS refers backscatter as detected from the multibeam data. Low backscatter indicates soft sediment and high backscatter a coarser or harder substrate.

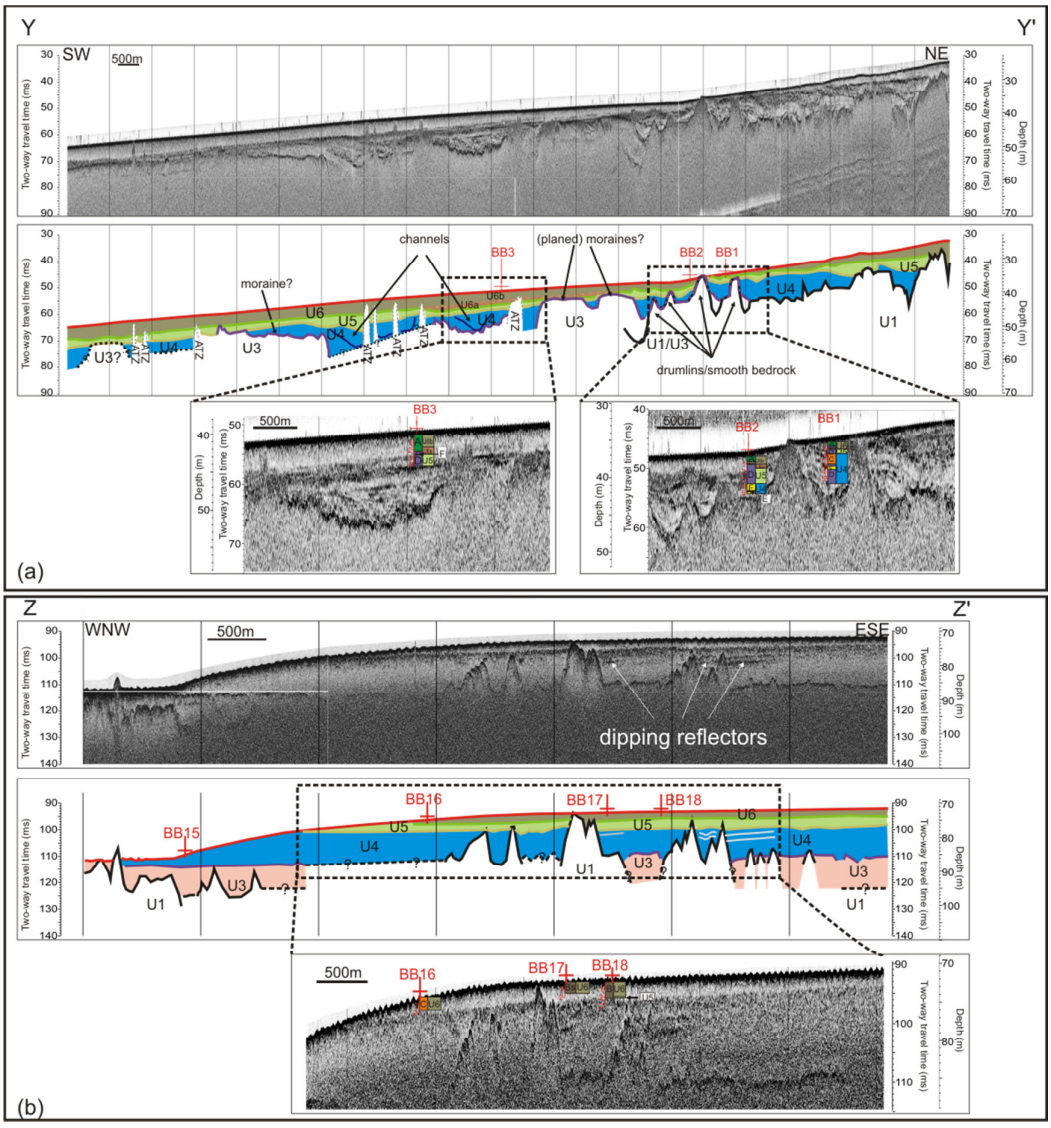

Figure 10. Relationship between seismic and core data showing position of cores on the seismic data together with the seismo-stratigraphic and bio-lithofacies interpretation. ATZ = acoustic turbidity zone.

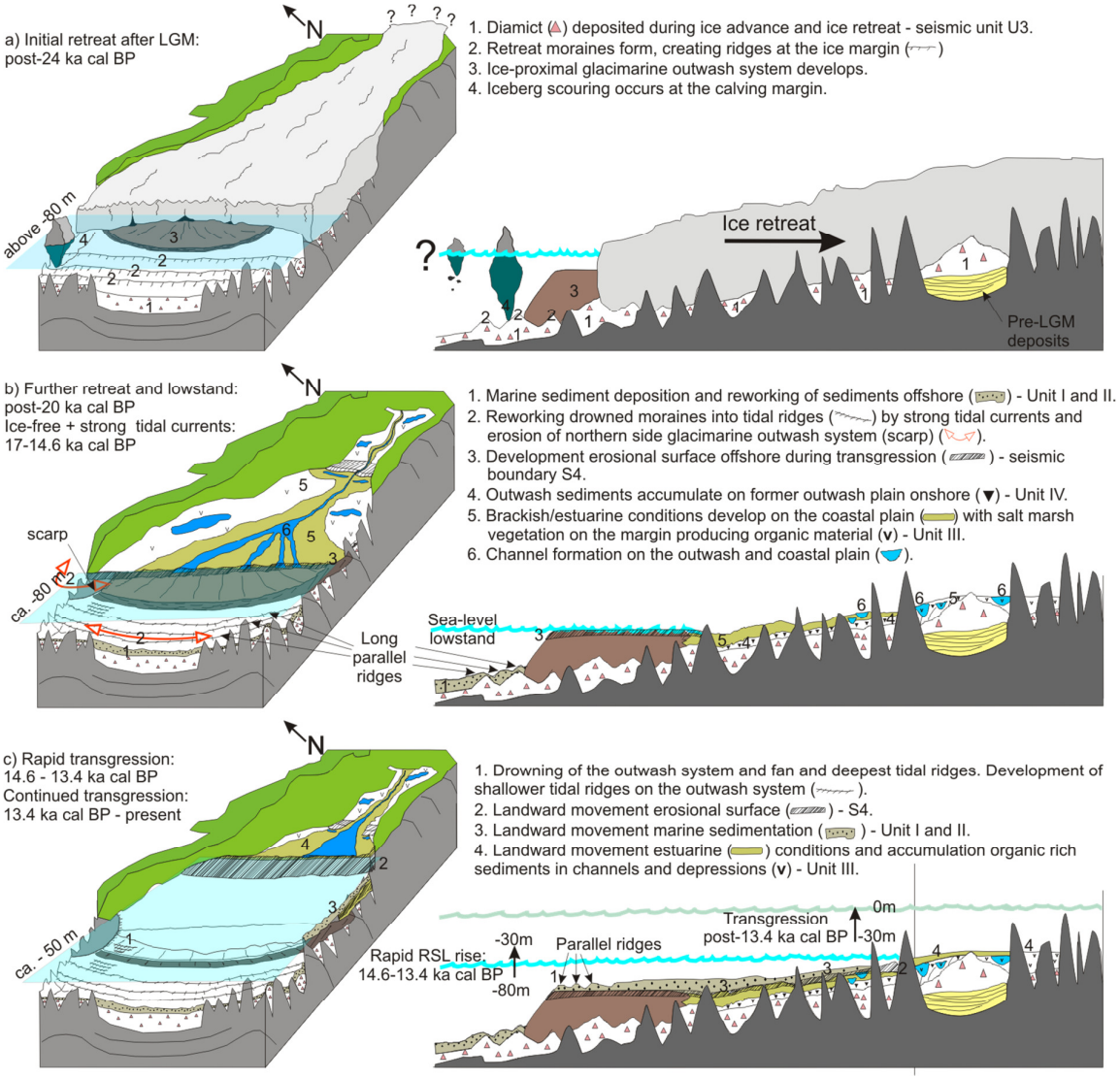

Figure 11. Proposed post-glacial sea-level evolution of Bantry Bay.

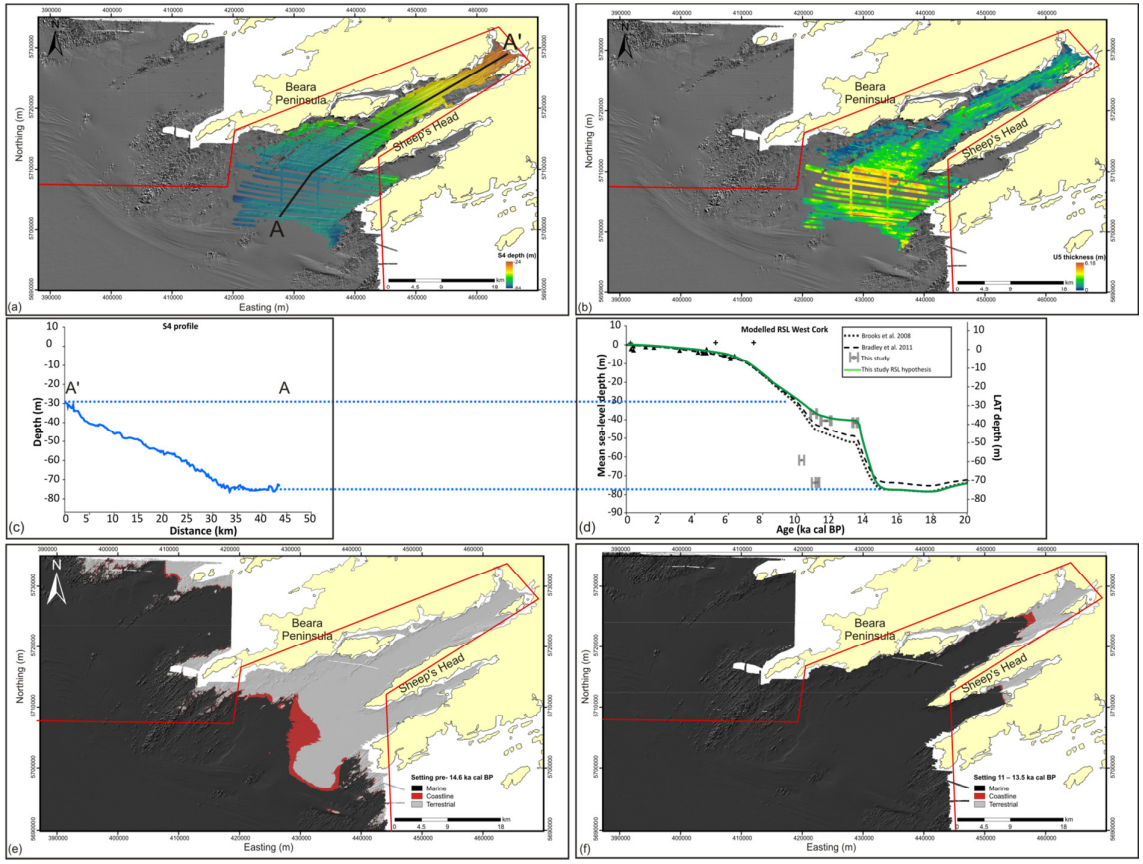

Figure 12. (a) Depth of the transgressive surface (S4) as traced from the seismic data; (b) the thickness of the basal transgressive unit (acoustic unit U5); (c) profile of the transgressive surface; (d) proposed RSL curve based on seismic and radiocarbon dates obtained through this research; (e) proposed position of the coastline during the pre-14.6 ka BP lowstand at c. 78 m mean sea-level depth (assuming an average of 3 m of sediments above the transgressive surface); (f) proposed position of the coastline during the 11 – 13.5 ka BP 'slowstand' at c. 40 m mean sea-level depth (assuming an average of 3 m of sediments above the transgressive surface).

Table 1: Selected species and depths for radiocarbon dating

Core	Publication code	Sample depth (cm)	Total depth (m below MSL)	Species dated	$d^{13}C$	^{14}C Age yrs BP	Calibrated age (Marine13) yrs BP
BB1	UCIAMS-149714	155 – 156	36.49 – 36.50	*Haynesina germanica*	4.2	9930 ± 35	10951 ± 182
BB1	UCIAMS-149715	160 - 161	36.54 – 36.55	*Haynesina germanica*	1.2	9965 ± 45	10982 ± 186
BB2	UCIAMS-149711	358 - 359	40.31 – 40.32	*Haynesina germanica*	0.5	10440 ± 30	11649 ± 289
BB2	SUERC-55680	363 - 364	40.36 – 40.37	Chenopod seed	-25.0	10104 ± 41	11691 ± 286
BB2	UCIAMS-149712	363 -364	40.36 – 40.37	*Haynesina germanica*	-2.8	10480 ± 30	11714 ± 290
BB2	SUERC-48863	460 - 461	41.33 - 41.34	*Elphidium excavatum*	-0.6	11845 ± 46	13360 ± 131
BB2	SUERC-48864	470 - 471	41.43 - 41.44	*Elphidium excavatum*	-1.4	11931 ± 47	13438 ± 151
BB18	UCIAMS-133553	182 - 183	73.65 - 73.66	*Quinqueloculina seminulum*	7.4	10135 ± 30	11184 ± 115
BB18	SUERC-48859	196 - 197	73.79 - 73.80	*Planorbulina mediterranensis*	-0.6	10008 ± 45	11031 ± 174
BB24	SUERC-48860	326 - 327	61.76 - 61.77	*Quinqueloculina seminulum*	0.1	9331 ± 45	10258 ± 152

Table 2: Summary of the main characteristics of each facies with depositional interpretation.

Bio-lithofacies	**Lithology**	**Top contact**	**Sedimentary structures**	**Shell content**	**Microfossils**	**Proportion broken tests**	**Munsell colour**	**Geographic distribution**	**Depositional interpretation**
A	silt or fine sand	Seabed	None	Varies from scattered to abundant with occasional shell hash layers	Abundant with *Bulimina marginata* dominating	Total: 29-33%; *A. becarrii*: 6-8%; *Bullimina species:* 9-11%; *E. excavatum*: 17%	2.5YR4/1-2 or 5Y4/1-2	Inner part of the bay	Low-energy inner shelf environment, with seasonal stratification in the water column.
B	Fine to medium sand	Sharp	Crudely laminated	Shell hash layers and occasional large shell fragments	Abundant with similar concentrations of *Asterigerinata mamilla, Milliolinella sp., Quinqueloculina sp., Textularia sagitula.* and *Cibicides lobatulus.*	41% at the top	2.5Y4/1	Predominantly outer part of the bay	High energy, open bay environment with possible reworking.
C	Massive fine to medium sand with complete shells or shell fragments	Gradual	None	complete shells or shell fragments	-	-	5Y4/1	Predominantly outer part of the bay	Rapid deposition in a high energy environment
D	Clay and sand layers	Sharp	Laminated, bioturbated, flaser bedding and organics material present	Few fragments and few large shells	*Asterigerinata mamilla, Cassidulina obtusa, Millionella sp*, *Cibicides lobatulus, Elphidium excavatum, Haynesina germanica* Some seeds.	Total: 28-30%; *A. mamilla:* 2-5%; *C. obtusa:* 2-10%; *C. lobatulus:* 3-4%;	5Y4-6/1	Inner part of the bay	Inter- to subtidal estuarine environment in inner Bay.

						E. excavatum: 2-8%			
E	Well rounded pebbles	Sharp	-	Some rolled shells	*Bulimina marginata, Cassidulina laevigata, Quinqueloculina* sp. and *Cibicides lobatulus*	33 – 46%		Two cores inner bay and one core exit Dunmanus Bay	High energy environment
F	Fine to medium sand, with abundant organic material	Sharp	Fining/coarsening upwards	few or no shell fragments	*Haynesina germanica, Elphidium excavatum, Milliolinella sp.* and *Cibicides lobatulus*	Total: 21-29%; *C. obtusa:* 8-10%; *E. excavatum:* 6%; *H. germanica:* low	5Y4-5/1	Inner bay and exit Dunmanus Bay	Inter- to subtidal estuarine environment, with possible tidal channels.

Table 3: Summary of the stratigraphic units showing the relationship between the seismo- and bio-lithofacies, with associated interpretation.

Stratigraphic Unit	**Seismo-facies**	**Bio-lithofacies**	**Palaeo-environment (based on Foraminifera)**	**Age**	**Interpretation**
I	U6 (U6b)	A/B (E)	Fully marine species dominate		Inner shelf conditions
II	U6 (U6a)	D (B/C)	Equal ratio of marine and estuarine species	Post- 11 ka cal BP	Transitional from estuarine lagoonal and shoreface to inner shelf conditions
III	U5	F – D (dominates) (offshore: B)	Equal ratio of fully marine versus marine/estuarine, with estuarine species becoming more abundant down-core	11 – 13 ka cal BP	Top: wave ravinement surface; Middle: estuarine shoreline at the mouth of the bay into estuarine lagoonal and tidal shoal in the inner bay; Bottom: transgressive surface
IV	U4	F (dominates) - D	Marine/estuarine species dominate, with a distinct presence of brackish species compared to overlying units	Pre- 13 ka cal BP	Offshore: sub-aqueous fan sediments; inshore: outwash plain with tidal channels and lagoonal muds; increasing marine influence towards the top of the unit
V	U3	N/A	N/A	LGM (26.5 – 19 ka cal BP)	Till
VI	U2	N/A	N/A	Pre-LGM	Sheltered estuarine or lacustrine environment
VII	U1	N/A	N/A	Devonian	Acoustic basement: Old Red Sandstone

Appendix 1: Summary of the position, depth and recovery of the vibrocore stations

Core no.	Length (m)	Water depth (LAT) (m)	Water depth (MSL) (m)	Latitude , Longitude
BB1	5.45	-33.34	-34.94	51°40.9657' , -9°33.4331'
BB2	4.9	-35.13	-36.73	51°40.7349' , -9°34.1857'
BB3	3.98	-38.01	-39.61	51°39.6305' , -9°37.7210'
BB4	1.64	-34.95	-36.55	51°40.8558' , -9°34.5007'
BB5	4	-31.72	-33.32	51°41.5058' , -9°32.8547'
BB6	2.95	-24.72	-26.32	51°42.5373' , -9°30.1874'
BB7	0.05	-84.29	-85.89	51°29.5570' , -10°09.5518'
BB8	0.1	-82.68	-84.28	51°29.5502' , -10°09.4863'
BB9	0.2	-81.23	-82.83	51°29.5303' , -10°09.2934'
BB10	1	-69.39	-70.99	51°29.0894' , -10°03.7909'
BB11	2.55	-66.69	-68.29	51°28.6140' ,-9°54.6647'
BB12	1.57	-70.07	-71.67	51°29.4144' , -10°05.3078'
BB13	1.83	-65.52	-67.12	51°28.7109' , -9°53.0773'
BB14	1	-72.24	-73.84	51°30.0545' , -10°06.7560'
BB15	0.1	-82.93	-84.53	51°30.7854' , -10°08.8685'
BB16	1.67	-72.50	-74.10	51°30.5874' , -10°07.0903'
BB17	1.46	-70.47	-72.07	51°30.4565' , -10°05.6895'
BB18	1.99	-70.23	-71.83	51°30.4043' , -10°05.3157'
BB19	1.87	-72.01	-73.61	51°30.9231' , -10°06.8474'
BB20	1.78	-69.97	-71.57	51°30.6488' , -10°04.3400'
BB21	4	-59.73	-61.33	51°30.7281' , -9°48.6547'
BB22	3.39	-68.30	-69.90	51°32.9506' , -10°04.8096'
BB23	2.27	-57.16	-58.76	51°31.2584' , -09°46.9034'
BB24	3.32	-56.90	-58.50	51°34.9369' , -09°50.2625'
BB25	2.67	-53.50	-55.10	51°35.7780' , -09°47.9339'

Appendix 2: Micropalaeontological summary.

The following is a list of foraminifera identified in the core including its occurrence and an environmental description of their habitat preference. The abundance has been split into 6 categories based on the maximum abundance a species has reached. These are <1%, 1-5%, 5-10%, 10-20%, 20-40% and >40%

	Abundance	**Distribution**	**Reference**
Suborder Textulariina			
Trochammina ochrea (Williamson)	<1%	Inner-shelf species. Clings to pebbles and seaweeds.	Murray, 1979
Textularia sagittula	20-40%	Epifaunal, shelf species and attaches to objects such as shells.	Murray, 1991 Murray, 2003
Textularia truncata (Höglund)	1-5%	Associated with *Textularia sagittula*	Murray, 1991
Suborder Spirillinina			
Spirillina vivipara Ehrenberg	5-10%	Epifaunal species, tends to cling to substrates such as pebbles and seaweeds. Marine, Inner-shelf species but can also be found living in estuary mouths.	Murray, 1979; Murray, 2003
Suborder Miliolina			
***Adelosina* type**	1-5%		
Cyclogyra involvens (Reuss)	5-10%	Inner-shelf species	Murray, 1971
Miliolinella subrotundra (Montagu)	20-40%	Epifaunal but living within the top 0.5 cm. Lives on sediment and marine plants. Tends to colonise estuarine mouths during favourable conditions. At its northern	Murray, 1971;

		limit in Britain and Ireland.	Murray, 1979; Murray, 2003
Prygo elongata (d'Orbigny)	<1%		
Pyrgo williamsoni (Silvestri)	<1%	Inner-shelf species.	Murray, 1971
Quinqueloculina sp	20-40%	Inner-shelf to marine group.	Murray, 1979
Suborder Lagenina			
Genus Fissurina	1-5%	A marine, shelf genus commonly found in muddy substrates. Dead tests can be transported and deposited into estuarine muds. All F*issurina* species listed below are grouped in the assemblage figure.	Murray, 1979
Fissurina lucida (Williamson)	1-5%	A stenohaline, shelf species	Murray, 1971
Fissurina marginata (Montagu)	1-5%	A shelf species.	Murray, 1971
Genus *Lagena*	1-5%	A marine, shelf genus commonly found in muddy substrates. Dead tests can be transported and deposited into estuarine muds during storm events. . All *Lagena* species listed below are grouped in the assemblage figure.	Murray, 1979
Lagena clavata (d'Orbigny)	1-5%	Shelf species.	Murray, 1971
Lagena doveyensis Haynes	<1%		
Lagena semistriata Williamson	1-5%	Shelf species.	Murray, 1971
Lagena sulcata (Walker and Jacob)	1-5%		
Genus Oolina	1-5%	A marine, shelf species commonly found in muddy substrates. . All *Oolina*	Murray, 1979

		species listed below are grouped in the assemblage figure.	
Oolina melo d'Orbigny	1-5%	A stenohaline, inner-shelf species.	Murray, 1971
Oolina williamsoni (Alcock)	<1%	Inner-shelf species.	Murray, 1971
Procerolagena clavata (d'Orbigny)	1-5%	Shelf species.	Murray, 1971
Suborder Rotaliina			
Ammonia batavus Hofker	1-5%	In this project all forms containing an umbilical boss is counted as *Ammonia batavus.* Tend to be located in marine, Inner-shelf environments.	Murray, 1979.
Ammonia beccarii (Linné)	10-20%	In this project all forms lacking an umbilical boss has been included as *Ammonia beccarii.* This group is commonly found in estuaries and brackish lagoons. This group is euryhaline and tolerate large (0-35‰) diurnal salinity range. Close to its northern limit in Britain and Ireland.	Murray, 1971; Murray, 1979
Asterigerinata mamilla (Williamson)	20-40%	Inner-shelf, marine species. Near to its northern limit in Britain and Ireland).	Murray, 1971; Murray, 1979
Bolivinellina pseudopunctata (Höglund)	5-10%	Marine, shelf species, but commonly transported and deposited in muddy estuarine sediments.	Murray, 1979
Brizalina difformis (Williamson)	1-5%	Shelf species, but can experience post-mortem transportation during storm events.	Murray, 1971
Brizalina spathulata (Williamson)	<1%	A stenohaline, shelf species, infaunal.	Murray, 1971; Murray, 2003

Brizalina variabilis (Williamson)	5-10%	Marine, inner-shelf species, sometimes transported and deposited in estuaries.	Murray, 1979
Bulimina gibba Fornasini	10-20%	Inner-shelf species.	Murray, 1971
Bulimina elongata d' Orbigny	10-20%	Inner-shelf species.	Murray, 1971
Bulimina marginata d'Orbigny	>40%	Infaunal, inner-shelf, marine species.	Murray 1979; Murray, 2003
Cassidulina laevigata d'Orbigny	10-20%	An outer shelf, infaunal species.	Murray, 1971; Murray, 2003
Cassidulina neoteretis Seidenkrantz	<1%		
Cassidulina obtusa (Williamson)	>40%	Shelf species, living in and on muddy substrates. Can occasionally be transported onto intertidal mudflats.	Murray, 2003
Cibicides lobatulus (Walker and Jacob)	20-40%	Marine, Inner-shelf species but dead tests are transported into estuary mouths. Species is epifaunal clinging to firm substrates including seaweeds and pebbles.	Murray, 1979
Elphidium crispum (Linné)	<1%	Marine, Inner-shelf species living at its northern limit in Britain and Ireland.	Murray, 1971; Murray, 1979
Elphidium excavatum (Terquem)	>40%	An inner-shelf species that can tolerate brackish conditions. High abundance of *Elphidium excavatum* is often found in areas experiencing high physical disturbance that received high loads of fresh organic material. Often used as a proxy for eutrophic conditions. Frequently found living in areas of strong water such as tidal flats or channels.	Murray, 1979; Murray, 1971; Nooijer et al, 2008
Elphidium gerthi Van Voorthuysen	1-5%	A marine, Inner-shelf species.	Murray, 1979

Elphidium incertum (Williamson)	1-5%	A marine, Inner-shelf species.	Murray, 1979
Elphidium magellanicum Heron-Allen and Earland	<1%	Tolerates brackish environments to open marine. Its habitat spans from hyposaline lagoons to innermost shelf.	Murray, 1971; Murray, 1979
Elphidium margaritaceum (Cushman)	1-5%	A marine, inner-shelf species.	Murray, 1979
Elphidium williamsoni Haynes	1-5%	Most common in brackish water and can tolerate a wide salinity range and variation.	Murray, 1979
Haynesina depressula (Walker and Jacob)	5-10%	Inner-shelf, marine species that can also live in estuarine mouths.	Murray, 1979
Haynesina germanica (Ehrenberg)	20-40%	A euryhaline species that can tolerate a large salinity range (0-35‰). Tends to be abundant in brackish environments including estuaries and lagoons.	Murray, 1979
Hyalinea balthica (Schöter)	<1%	A shelf species	Murray, 1971
Nonionella turgida (Williamson)	5-10%	An infaunal, shelf species.	Murray, 1971; Murray, 2003
Patellina corrugata Williamson	1-5%	Marine, inner-shelf species but can also be found living in estuary mouths. Species is epifuanal clinging to firm substrates including seaweeds and pebbles.	Murray, 1979
Planorbulina mediterranensis (d'Orbigny)	5-10%	Marine, inner-shelf species but dead test can be transported into estuary mouths. Species is epifuanal clinging to firm substrates including seaweeds and pebbles.	Murray, 1979
Rosalina anomala Terquem	5-10%	Inner-shelf, marine species. Grows clinging to seaweed and firm substrates.	Murray, 1979
Rosalina williamsoni (Chapman and Parr)	<1%	Inner-shelf, marine species.	Murray, 1979
Stainforthia fusiformis (Williamson)	1-5%	Marine species, but commonly transported and deposited in muddy estuarine sediments. Also documented as *Fursenkoina fusiformis* or *Virgulina fusiformis.*	Murray, 1979

Trifarina angulosa (Williamson)	<1%	Marine, shelf species that can sometimes be transported into estuaries.	Murray, 1979
Planktonic species			
Globigerina bulliodes d'Orbigny	1-5%	Cold temperate to subpolar species.	Murray, 1971
Globigerina pachyderma (Ehrenberg)	1-5%	Cold temperate to subpolar species.	Murray, 1971

Appendix 3. Schematic representation of abundance and palaeo-environmental classification of all identified foraminifera.